

Received November 9, 2018, accepted November 24, 2018, date of publication November 28, 2018, date of current version December 31, 2018.

Digital Object Identifier 10.1109/ACCESS.2018.2883788

# User Influence on Mobile Terminal Antennas: A Review of Challenges and Potential Solution for 5G Antennas

**RIZWAN KHAN<sup>1</sup>**, (Student Member, IEEE),  
**AZREMI ABDULLAH AL-HADI<sup>1</sup>**, (Senior Member, IEEE),  
**PING JACK SOH<sup>1</sup>**, (Senior Member, IEEE),  
**MUHAMMAD RAMLEE KAMARUDIN<sup>2</sup>**, (Senior Member, IEEE),  
**MOHD TARMIZI ALI<sup>3</sup>**, (Senior Member, IEEE), AND **OWAIS<sup>4</sup>**

<sup>1</sup>School of Computer and Communication Engineering, Universiti Malaysia Perlis, Arau 02600, Malaysia

<sup>2</sup>Centre for Electronic Warfare, Information and Cyber, Cranfield Defence and Security, Cranfield University, Defence Academy of the U.K., Shrivenham SN6 8LA, U.K.

<sup>3</sup>Antenna Research Centre, Fakulti Kejuruteraan Elektrik, Universiti Teknologi Mara, Shah Alam 40450, Malaysia

<sup>4</sup>Electrical Engineering Department, COMSATS University Islamabad, Abbottabad 22060, Pakistan

Corresponding authors: Azremi Abdullah Al-Hadi (azremi@unimap.edu.my) and Muhammad Ramlee Kamarudin (Ramlee.Kamarudin@cranfield.ac.uk)

This work was supported by the Ministry of Science, Technology and Innovation under Science fund under Grant 01-01-015-SF0258.

**ABSTRACT** This paper presents a comprehensive review of mobile terminal antenna researches performed in the past seven years and the current challenges related to the user's influence on the performance of fifth generation (5G) terminal antennas. The main challenges for the designing of mobile terminal antennas are to meet the compact size requirements of built-in structures and their multiband capabilities. The antenna design techniques that are used to achieve broader operating bandwidths with smaller antenna dimensions will be first discussed. This is followed by the effects of user interactions with the head/hand for mobile antennas in terms of radiation efficiency and, consequently, the correlation of multiple input multiple output (MIMO) antenna systems. The ultimate aims of this paper are as follows: 1) to highlight the different frequencies of mobile terminal antennas for different applications; 2) to highlight mobile terminal antennas that have been developed for 5G application; 3) to study and discuss the effects of user's hand on 5G mobile terminal antennas; and 4) to discuss the research gap, issues, and challenges in the field of user's effects on mobile terminal antennas for 5G applications. In addition to that, an investigation of the users' hand effects on two MIMO mobile terminal antennas operational in the sub-6-GHz 5G band is presented. This investigation performed using two MIMO antennas is an attempt to formulate guidelines on efficient mobile terminal antenna design in the presence of user's hand in C Band (from 3.4 to 3.6 GHz) and LTE-U Band 46 (from 5.15 to 5.925 GHz).

**INDEX TERMS** Electromagnetic influence of users, mobile terminal antennas, multiband antennas, MIMO antennas.

## LIST OF ABBREVIATION

3G 3rd Generation

4G 4th Generation

5G 5th Generation

AD1 Antenna Design 1

AD2 Antenna Design 2

AE1 Antenna Element 1

AE2 Antenna Element 2

CCE Capacitive Coupling Element

DCS Digital Cellular System

ECC Envelop Correlation Coefficient

FS Free Space

GSM Global System for Mobile communications

IM Impedance Matching

ITU International Telecommunication Union

LB Lower Band

LH Left Hand

LTE-A Long Term Evolution-Advance

MC	Mutual Coupling
ME	Multiplexing efficiency
MIMO	Multiple input multiple output
MITT	Ministry of Industry and Information Technology
PCB	Printed Circuit Board
PCS	Personal Communications Service
PIFA	Planar Inverted F Antenna
RE	Radiation Efficiency
RH	Right Hand
RR	Radio Regulation
SAR	Specific Absorption Rate
SISO	Single Input Single Output
UB	Upper Band
UMTS	Universal Mobile Telecommunications System
UHF	Ultra High Frequency
WC	With Casing
WiMAX	Worldwide Interoperability for Microwave Access
WLAN	Wireless Local Area Network
WRC	World Radio Conference

## I. INTRODUCTION

Over the last three and a half decades, advancements in cellular communication standards have significantly affected the development of terminal antennas. Two major factors have been involved in this evolution. Firstly, is the users' demand, which is mainly composed of aesthetical and ergonomic considerations, and secondly, the introduction of new spectrums in line with the evolving regulatory standards. Therefore, one of the most challenging requirements for designers of mobile wireless communication systems is the design of antennas. The rapid growth of mobile systems towards 5G requires antennas to be wideband, multiband or even ultra wideband to enable coverage interoperability of mobile services and to reduce system complexity. Other challenges for mobile terminal antennas include size compactness, ease of integration into the handheld chassis and coexistence with and the support for multi-antenna operation and MIMO systems. MIMO is one of the major enablers of 5G technology in achieving up to 100 times of bandwidth relative to 4G and LTE-Advance (LTE-A) systems. This technology offers increased system capacity with additional number of antenna elements, without the need for additional power or frequency spectrum. A well performing MIMO system requires high efficiency for each element and a low correlation between them [1], [2]. However, this requires sufficient inter-element spacing, which is difficult to find in mobile terminals as they are ideally designed to be compact and wideband. This is to ensure that new smart phones are backward compatible, supporting technologies prior to the fourth generation (4G) for global coverage and roaming using the same device [3].

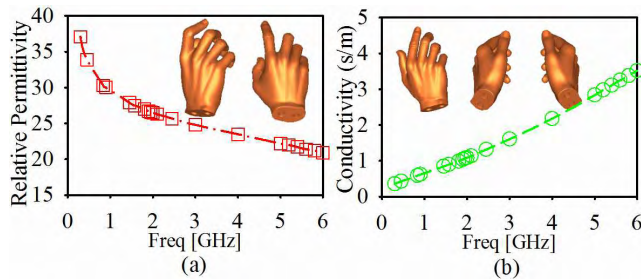
Planar inverted-F antenna (PIFA) is one of the most commonly used internal antennas in the handheld segment (such as mobile phones) due to its ease of fabrication, low profile and potentially low cost [4]. Another most commonly used

antenna type in mobile phones is the monopole antenna. Such antennas started to gain popularity upon the introduction of the new 3G, 4G and 5G frequency bands, as they are able to offer broader bandwidth relative to PIFAs [4]. Additional parasitic elements such as capacitive coupling elements (CCE) are typically used in mobile terminal antennas to excite inherently non-resonant structures. Their structure and location are carefully designed to excite particular wave modes on the ground plane in a systematic manner [5], [6].

Furthermore, there are significant on-going standardization activities to identify common usable spectrums across many countries to enable global roaming and economy of scale. The World Radio Conference 2015 (WRC-15) revised the Radio Regulations (RR) and the International Telecommunication Union (ITU) treaty for radio spectrum [7] identified and deployed 4G spectrum in many parts of the world. As 5G standards and technologies continues to mature, bands already in use for 4G will also evolve as 4G to 5G transition bands [8]. One of such realistic bands announced is the C-band between 3.4 and 3.6 GHz [7]. In early 2015, LTE band 42 (from 3.4 to 3.6 GHz) was initially defined as the band of interest for China [9]. This was revised in November 2017 by China's Ministry of Industry and Information Technology (MITT), which officially reserved the 3.3 to 3.6 GHz and 4.8 to 5 GHz for the country's 5G service, with the 3.3 to 3.6 GHz band being intensively investigated as a pioneering band for realizing 5G MIMO [10], Europe (from 3.4 to 3.8 GHz) [11], and Korea (from 3.4 to 3.7 GHz) [12]. Besides that, another potential sub-6 GHz frequency band for 5G is the LTE band 46 (from 5.15 to 5.925 GHz), also known as the unlicensed LTE band (LTE-U).

Besides designing operational MIMO antennas in these sub-6 GHz bands, an additional step in ensuring operation in the design procedure is to study the users' influence on the performance of mobile terminal antennas. The antenna design process for mobile terminals must also account for the effects of its housing for optimized MIMO performance. Besides that, upcoming regulatory standards are expected to incorporate performance evaluation of these terminals with hand models by manufacturers. This has propelled research interests in quantifying the interaction between radiating elements in wireless terminals and biological tissues of users. Such concern is obvious given the fact that the parts of the body (head, hand or body) located in proximity of the terminal causes increase in absorption losses, impedance variation, radiation pattern deterioration and detuning of resonance frequency. Moreover, the resulting absorption losses varies depending on the frequency due to the different permittivity of user's hand with frequency, besides their hand grips, as shown in Fig. 1 [13]. This is due to the different penetration depths resulting from the use of different frequency bands.

This paper is organized as follows. An overview of mobile terminal antennas operating at different frequency bands is first discussed. This is followed by a critical review of the recent publications on mobile terminal for 5G application over last seven years. From this review, current research



**FIGURE 1.** Skin properties according to different frequencies, (a) relative permittivity and (b) conductivity [12].

issues and challenges related to the user's hand effects within the sub-6 GHz 5G bands will be identified and discussed in detail. Finally, a potential solution is presented via an evaluation work on two different antennas operating in the sub-6 GHz bands is performed in close vicinity of user's hand and presented. The concluding remarks presented at the end of this work include future strategies to alleviate these effects throughout the design process.

## II. SISO ANTENNAS IN MOBILE TERMINALS

Throughout the years, mobile phones have undergone significant changes in terms of size, shape and functionalities. With each development, the smartphones are generally aimed with more compact sizes and lighter weights for improved mobility. Such specification requires antennas to be designed to be broad- and/or multiband within a smaller available volume. The following section will present the recent literature regarding wide-band and dual band Single Input Single Output (SISO) antenna for mobile terminal.

### A. WIDE BAND AND DUAL BAND MOBILE TERMINAL ANTENNAS

Due to lack of wide band and dual band SISO antennas in the past seven years, several designs will be summarized in this section. It is also worthy to mention that a previous review on mobile terminal antennas was presented in [3]. Wide band antennas for mobile terminal have been studied in [14]–[21] since 2011. Instead of implementing contacting feeds used in conventional PIFAs, a coupled feed structure is used to improve the bandwidth in [14], resulting in an operation from 0.82 to 3 GHz. Next, a monopole sleeve antenna is proposed in [15].

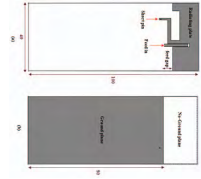
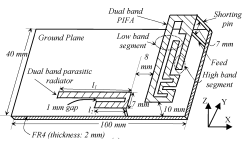
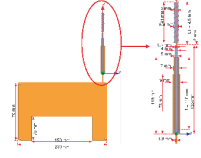
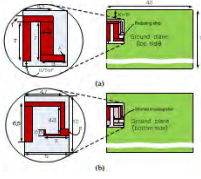
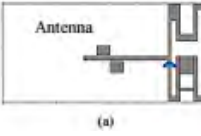
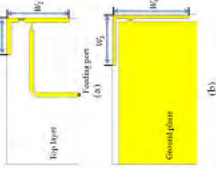
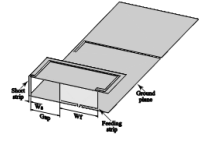
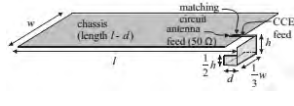
An enhanced operational bandwidth from 0.3 GHz to 0.7GHz is achieved in this design by adding a conical sleeve and helical structure on the top of the antenna. Meanwhile, a wideband planar monopole antenna for mobile terminals is proposed in [16]. The increase in bandwidth is achieved by connecting two arms of a U-shape radiator using two parallel radiating strips. Next, the wideband operation of a PIFA antenna is enabled in [17] by introducing a slot on the top of radiating element. Further down the frequency spectrum, an internal broadband antenna is designed for the lower Ultra High Frequency (UHF) band in [18], resulting in its operation across all lower frequency cellular bands,

from 0.7 to 0.96GHz. To enable dual band operation, combining the operation of two radiators with different electrical lengths is a typical method used. An example is provided in [19] for a dual-band PIFA implementing a longer radiating element for lower frequency resonance and a shorter element for higher resonance. Besides that, a dual-band parasitic element is also designed to reduce the effects of ground plane, this leads to the reduction in the electromagnetic energy deposited in the hand phantom and hence lower SAR. Next, a contour integrated dual band compact antenna elements for low profile mobile terminals is presented in [20]. This design utilizes a multiple resonating structure to result in a dual band operation at 2.4 and 5.5GHz. Additional resonance for antennas may also be introduced by implementing coupling strips, as seen in [21]. A dual-band antenna with shorted coupling strips is presented for mobile terminals by using this technique. This additional resonance combined with the existing operating band to enable a wideband characteristic for the proposed antenna. Antennas from [14]–[21] and their bandwidths are summarized in Table-1.

### B. MULTI BAND MOBILE TERMINAL ANTENNAS

Next, recent published investigations on multiband mobile terminal antennas for different bands are presented and discussed in this section [22]–[31]. Note that these antennas are being integrated internally in the housing of the mobile terminals, and thus can be used as a resonant cavity to improve radiation. Moreover, another important trend is that mobile terminals are increasingly integrated with multimedia capabilities since the late 1990s [3]. The first antenna in [22] combines different wave modes of the antenna and chassis to achieve multiband antenna without any matching circuits or magneto-dielectric materials. Another use of modes for this purpose is a dual zeroth-order resonance by using composite right and left handed metamaterial line [23]. Next, an internal quad band printed monopole antenna for an oval-shaped mobile phone is presented in [24]. Three different slits are integrated onto the oval-shaped radiating elements to obtain operation in the four mobile communication bands. Besides the concept of slots and slits, the combined use of the electric and magnetic monopole antenna is also used to enable multiband operation for mobile phone application. This technique is proposed in [25], where a new magneto-electric monopole antenna is designed using two horizontal slot monopoles and a vertical monopole with a shorting strip to allow a dual-band and wideband operation. Besides that, the use of simple parasitic elements for a printed antenna is shown to be able to add to the number of resonance in [26]. This is done by using two simple metal stubs to separate three resonances to result in operation across six different cellular bands. Meanwhile, a method of hybrid loop on a printed PIFA for mobile terminals is presented in [27] to operate in a multi-band characteristic. Another concept of utilizing additional strip with the radiating element multiband operation can be achieved as shown in [28]. This additional strip is etched from the no-ground area located near the radiating element.

TABLE 1. Summary of SISO antennas [14]–[21].

Ref	Antenna Design	Bandwidth [GHz]	Ref	Antenna Design	Bandwidth [GHz]
[14]		0.82 - 3	[18]		0.88 - 0.96 and 1.85 - 1.99
[15]		0.3 - 0.7	[19]		2.39 - 2.49 and 5.07 - 5.88
[16]		1.33 - 3.5	[20]		2.27 - 2.52 and 5.29 - 5.53
[17]		0.8 - 0.97 and 1.5 - 5.9	[21]		0.7 - 0.96

Similarly, the multiband behavior of the antenna in [29] can also be introduced by etching circular slots on the radiating element itself. Another example of this method is by using multiple slots and meandered strips as shown in [30]. Besides that, several resonant branches were designed in [31] to obtain multiband feature, whereas a coupling element is used to miniaturize the size of the antenna. The designs and their operating frequencies proposed in [22]–[31] are summarized in Table 2.

From this section, it is observed that to enable wideband operation to fulfill cellular requirements, the useful techniques includes etching slots on their radiating elements. On the other hand, others have proposed the insertion of parasitic elements to result in additional bands. However, a drawback of this technique is the added design complexity and larger sizes, which may cause interference with other circuitry located on the mobile terminal chassis.

III. MIMO ANTENNAS FOR MOBILE TERMINALS

The deployment of MIMO systems ideally requires the employment of multiple antennas at both the base

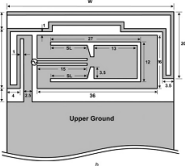
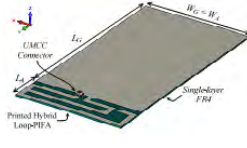
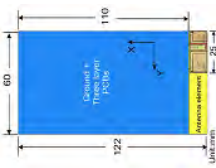
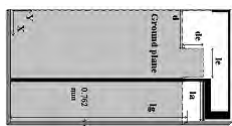
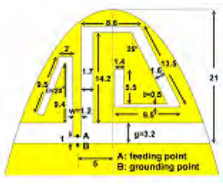
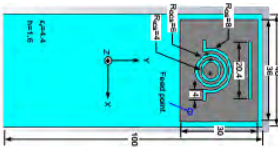
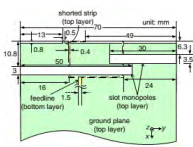

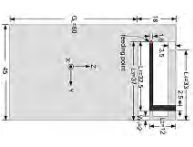
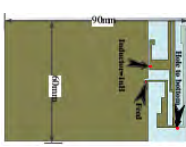
stations and mobile terminals. This enables a linear increase in channel capacity with the additional number of antennas. A recent review on MIMO antennas for mobile terminals was presented in [2], whereas the following section discusses more details of the literature not covered in [2].

A. WIDEBAND MOBILE TERMINAL ANTENNAS

MIMO antennas are considered as an integral part of LTE and LTE-A systems. Moreover, the trend of integrated mobile terminals in recent years increases the number of operating frequency bands to operate across different wireless applications. One way to reduce the number of antenna elements and to provide coverage for different wireless standards is to use wide band antennas. Different wide bands MIMO have been published in last seven years. While a part of these literature are found in [2], the remaining papers [32]–[47] will be further discussed.

Wideband diversity antenna for mobile terminals are presented, operating from 1.8 to 4.6 GHz in [32], and from 1.85 to 2.31GHz in [32]. In [32] diversity is achieved

TABLE 2. Summary of multiband SISO antennas [22]–[31].

Ref	Antenna Design	Bandwidth [GHz]	Ref	Antenna Design	Bandwidth [GHz]
[22]		0.46 - 785, 880 - 980 and 1.45 - 1.49	[27]		0.834 - 0.907, 1.985 - 2.845 and 3.253 - 3.593
[23]		0.824 - 0.96 and 1.710 - 2170	[28]		0.70 - 0.96, 1.75 - 2.3 and 3.1 - 4.38
[24]		0.824 - 0.96 and 1.71 - 1.99	[29]		2.08 - 2.17, 3.55 - 3.65, 4.88 - 4.94 and 5.68 - 5.76
[25]		0.704 - 1.04 and 1.56 - 2.46	[30]		0.45 - 0.474, 0.86 - 1.04, 1.7 - 2.43 and 2.5 - 2.71
[26]		0.89 - 0.96, and 1.4 - 2.7	[31]		0.87 - 0.96, 1.7 - 2.2 and 2.49 - 2.72

by utilizing two orthogonally oriented quasi-complementary antennas formed using a combined electric dipole and a magnetic slot. They are located at the separate ends of a mobile terminal chassis. Meanwhile, a concept of two symmetric slot-monopole-hybrid elements was used to achieve diversity performance of the antenna in [33]. A similar concept of combining the electric dipole and a square magnetic slot a special diversity is achieved with in the bandwidth between 2.0 and 5.6 GHz in [34]. Finally, an antenna with EM-coupled feed is also used to obtain dual band operation [35].

Several decoupling method have also been introduced for multiple wide band antennas in [36]–[47]. Neutralization line technique is used to decouple these antennas in [36]–[40].

A thin neutralization line is inserted between two antennas to reduce mutual coupling. Another method for this purpose is by inserting a parasitic element between the antenna elements [41], [42]. Ground current modification is also an alternative way to decrease the mutual coupling between antenna elements [43]–[45]. One of the most recent techniques is by designing a metamaterial band decoupling structure to minimize mutual coupling. The decoupling component is made of sub-wavelength metal-air layers, which can be treated as a singular medium operating over a broad frequency band [46]. Finally, another new method to decouple antennas is by designing a balanced and unbalanced antenna to achieve high level of isolations [47].





## B. DUAL BAND AND MULTIBAND MOBILE TERMINAL ANTENNAS

An effective method to minimize the number of antenna elements in a mobile terminal is to design dual- or multi-band antennas. This is for the same purpose, which is to provide coverage of across different wireless applications. Investigations performed on dual- and multiband antennas includes the mutual coupling reduction techniques proposed in [48]–[54]. An impedance transformer based on a T-shaped slot is used for to minimize mutual coupling between two different antennas operating in dual and wideband modes in [48]. Besides that, defected ground structure is also an effective way for the same purpose, as seen in the dual band MIMO in [48]. Meanwhile, ground slots and the introduction of parasitic elements can also enable mutual coupling reduction in dual band antennas [49]–[51]. To ensure compactness of a dual band MIMO antenna system, differently shaped antenna elements are designed in [52] and [53], resulting in the antenna miniaturization of up to 50 %. The next method in enabling size compactness is by using contour integration on a compact two-element MIMO antenna in [54] for dual band operation. Another method is by wrapping the antenna on a spacer, which is located at the edge of the mobile chassis [55]. In this work, a single antenna element is fed by dual port to enable dual band MIMO operation.

On the other hand, several multiband antennas have also been proposed for the purpose of operating in more than two cellular bands [56]–[60]. The first is a multiband diversity antenna designed using branches of a folded monopole. At least one of the branch is terminated with a rectangular patch, resulting in a multiband behavior [56]. Besides diversity, multiband antennas can also be designed by introducing different branches in the radiating elements, or by using stub elements, loop elements and meander lines [57]–[60]. In decoupling multiband antennas, ground current modification and decoupling slots are more often used [61], [62]. A complete review on mutual coupling techniques for MIMO antennas can also be found in [63].

In this section, several wide, dual- and multiband antennas for MIMO have been studied, including methods to decouple multiple radiating elements in these antennas. While most of the reviewed techniques have been proven effective, it can be concluded that the use of neutralization line can only be effective for single band antennas. However, an introduction of t-shaped transformer on the ground plane is useful for to decouple both single and dual band antennas. For the case of multiband antenna ground perturbation and decoupling slot lines are useful to reduce the mutual coupling.

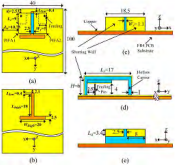
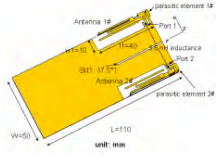
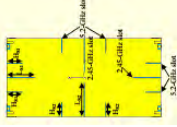
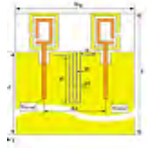
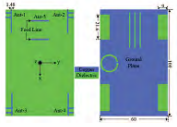
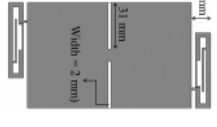
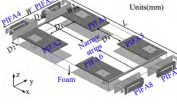

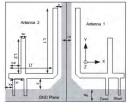
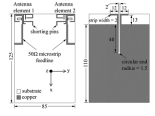
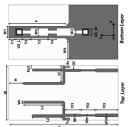

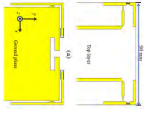
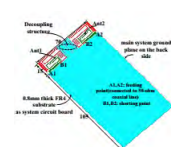
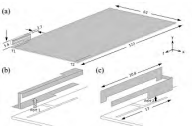
## IV. METAL-RIMMED MOBILE TERMINAL ANTENNAS

In recent years, the antenna and mobile phone industry are increasingly designing smartphones with metal-rims and big display screens. Such metal-rimmed smartphones offers excellent mechanical robustness and good aesthetic appearance. Despite that, the existence of such structures poses a significant challenges for engineers due its undesirable

impact on antenna performance, especially when the continuous metal-rim type is selected for use. Due to the significance of this issue, research on metal-rimmed antenna is increasingly investigated and reported, which may warrant a separate review on this topic. In this survey, the main focus on the effects of the user's hand is maintained, and relevant literature on this aspect for metal-rimmed antennas is discussed in the following paragraphs.

Recent studies the user's effect on the performance of metal-rimmed mobile terminal antenna and have been presented in [64]–[71]. Thus far, there very limited number of studies on the effects of the users for metal-rimmed mobile terminal antennas, and existing studies are limited to designs operating in the cellular band below 3 GHz, specifically, for the GSM 850/900, DCS, PCS, UMTS 2100, LTE 2300/2500 bands. In [64] and [65] a multiband, dual loop antenna surrounded by a continuous metal rim is presented. Three different user's hand grips were used in this study, and it was found that efficiency of the proposed antenna degraded from 75% to between 23% and 32% due to the proximity of the users' hand. On the other hand, the work in [65] further considered an additional scenario where the user held the antenna with two hands. In case of two hands, efficiency degraded approximately 15% and 25%. Next, the researchers in [66] presented a parallel dual-loop antenna embedded on the system's ground. A L-shaped coupled feed line with addition matching networks is used to excite a multiple loop resonant modes. A maximum efficiency reduction of below 20% and 40% is observed for LB and UB in three user's hand grips on the proposed antenna. Meanwhile, a narrow frame antenna with hybrid multimode for a metal rimmed smart phone is presented in [67]. A three grounded patches with a small gap were used to connect the metal to the system's ground plane. A SAR values were analyzed for the proposed antenna using the human head model instead of hands. It is observed that the SAR values for the proposed antenna are well below the regulated limits and efficiency values are also within the limits for practical use of the antenna. In [68], an inverted-F mobile terminal antenna surrounded by a metal rim with two slots is proposed. To obtain a high radiation performance, the metal rim is cut into three parts, resulting in the proposed antenna's operation in a multiband mode. However, due to direct influence of the user's hand, its efficiency degraded to about 40 % in all operating bands. Finally a reconfigurable multiband antenna is proposed in a narrow-framed, metal-rimmed smartphone in [69]. In this design, reconfiguration is achieved by using a PIN diode to enable the antenna operation in two states. Multiple user's scenarios are also used to investigate its effects on antenna performance, and it is noticed that antenna efficiency degraded to an average of 30% when held in the user's hand scenario. Despite that, the SAR values maintained below the allowable limits, indicating that the antenna can be used in practice. Besides this, metal frames can also be designed to act as the antenna radiating element. This is done in [70], where full LTE band operation is achieved by integrating inductors,

TABLE 4. Summary of MIMO dual and multiband antenna [48]–[62].


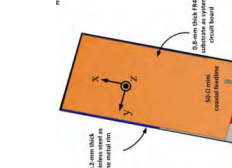
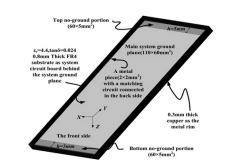
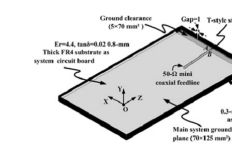
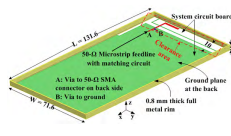
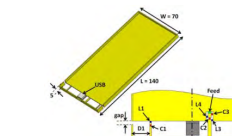
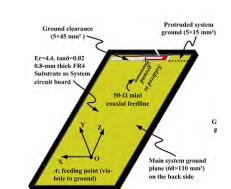
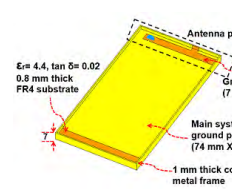
Ref	Antenna Design	Bandwidth [GHz]	Ref	Antenna Design	Bandwidth [GHz]
[48]		2.4 - 2.48, and 3.4 - 3.6	[56]		0.746 - 0.798, and 1.71 - 2.7
[49]		2.35 - 2.6 and 5.1 - 5.3	[57]		1.924 - 2.2, 2.836 - 3.235 and 5.629 - 5.743
[50]		1.93 - 2.05 and 3.99 - 4.23	[58]		0.68 - 0.912, 1.92 - 2.203 and 2.38 - 3.603
[51]		2.6 - 2.8 and 3.4 - 3.6	[59]		0.88 - 0.96, 1.75 - 1.87, 2.3 - 2.4 and 2.4 - 2.5
[52]		0.58 - 0.92 and 2.955 - 3.13	[60]		0.826 - 1.005, 1.527 - 2.480, 3.436 - 3.690 and 5.34 - 5.725
[53]		0.803 - 0.823 and 2.44 - 2.90	[61]		0.824 - 0.960 and 1.71 - 2.690
[54]		2.34 - 2.5 and 5.18 - 5.5	[62]		0.704 - 0.787, 0.88 - 0.96 and 1.8 - 2.69
[55]		2.4 and 5.0			

band pass filter and an additional matching network. The antenna performance is then analyzed in talk mode, and this operation resulted in the antenna efficiency degradation to

between 10.3% and 17.5% in the lower band (0.698 to 0.96) and between 14 % and 30% for upper band (1.71 to 2.69). Besides matching circuits, varactor diodes can also be used



TABLE 5. Summary of metal-rimmed antennas [64]–[71].

Ref	Antenna Design	Bandwidth [GHz]	Ref	Antenna Design	Bandwidth [GHz]
[64]		0.824 - 0.96 and 1.71 - 2.69	[68]		0.824 - 0.96 and 1.71 - 2.69
[65]		0.798 - 0.968 and 1.44 - 2.95	[69]		0.824 - 0.96 and 1.71 - 2.69
[66]		0.824 - 0.96 and 1.71 - 2.69	[70]		0.698 - 0.96 and 1.71 - 2.69
[67]		0.822 - 0.965 and 1.59 - 2.91	[71]		0.698 - 0.96 and 1.71 - 2.69

to miniaturize the size of antenna as demonstrated in [71]. In this work, a reconfigurable open slot antenna is placed at the bottom chassis of the mobile terminal and is integrated with a metal rim. The structure’s performance is studied using both user’s hand and a head phantom. A significant total efficiency reduction is observed for the antenna, which was 18% initially, degrading to between 6% and 10% (in the lower band) from 0.698 to 0.96 GHz and between 6% and 18% (in the upper band) from 1.71 to 2.69 GHz when the user’s finger touches the metal rim slot. However, SAR values produced are still below the regulated limits.

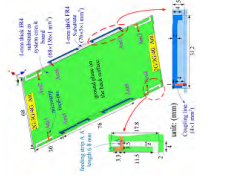
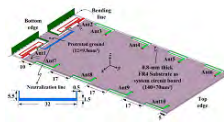
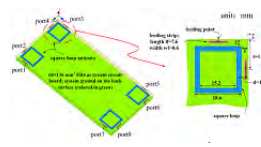

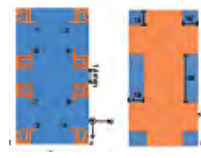
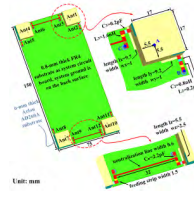
From this section it is noticed that the use of metal-rimmed antennas is a promising solution to achieve a multiband operation. This can be simply implemented by introducing several ground patches and gaps onto the outer metal rim. Besides that, another method is to use the entire metal rim as a radiating element, which further facilitates antenna miniaturization. Another creative method to make the most of metal rims is separate them into individual parts, such as using slits to form multiple radiators (such as IFAs) to excite multiple resonant modes. Besides that, the implementation of coupling strips

may also contribute to such aim. In summary, researches thus far have been focused on the design of the metal-rimmed antenna and in capitalizing such structure. However, the main challenge remains for such structure, which is to address the performance deterioration caused by the user’s hand.

### V. MOBILE TERMINAL ANTENNA FOR 5G APPLICATION

The rapid demand increase of mobile data presented by the wide use of smartphones has been compounded by the bandwidth spectrum shortage in recent years [72]. Wireless devices can typically operate between 700 MHz and 2.6 GHz [73]. Due to this, the implementation of the 4G cellular networks, and research and standardization activities on the 5G technologies are rapidly progressing both in academia and industry [74]. Due to the near-standardization of 5G frequencies, literature on terminal antenna designs are limited, and available ones will be discussed in this section [75]. The first is a substrate integrated magneto-electric dipole antenna proposed in [75]. This design operated from 4.98 to 6.01 for 5G. A H-shaped ground plane is also introduced to miniature the antenna in its operating band. Future MIMO

TABLE 6. Summary for 5G mobile terminal antennas [78]–[83].

Ref	Antenna Design	Bandwidth [GHz]	Ref	Antenna Design	Bandwidth [GHz]
[78]		2.55 - 2.65	[81]		0.824 - 0.96 1.71 - 2.69 and 3.4 - 3.6
[79]		2.55 - 2.65	[82]		3.4 - 3.6
[80]		1.8 - 1.92, 2.3 - 2.4 and 2.54 - 2.62	[83]		3.4 - 3.6

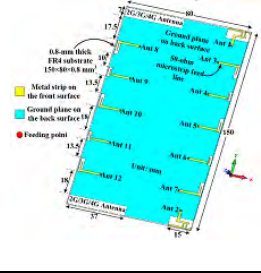
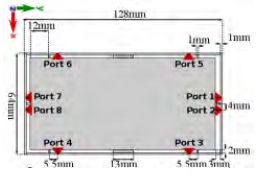
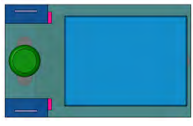
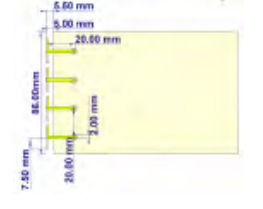
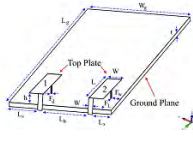
applications in mobile terminals are likely to favor wide-band antennas, as demonstrated in [76] and [77]. In [76], a wideband printed MIMO antenna operational from 3 to 9 GHz band for 5G is proposed. Meanwhile, a circular polarized antenna for 5G is presented in [77] with an operational bandwidth of 11.08 %, ranging from 3.58 to 4 GHz. Next, a dual polarized hybrid eight-antenna array in the 2.6 GHz band (from 2.55 to 2.65) for 5G MIMO is proposed in [78] and [79]. Meanwhile, in [80], an eight element printed MIMO antenna system for a 5G mobile terminal operating between 2.54 and 2.62 GHz was investigated. The compatibility between 4G and 5G hardware is the main feature of the antenna module presented in [81]. On the other hand, a compact four port MIMO mobile terminal antenna is investigated in [82] for 5G applications. The most recent work proposed a tri-polarized 12-element MIMO array antenna for 5G application, where the antenna is operational from 3.4 to 3.6 GHz [83]. Finally, the researchers in [81]–[83] have indicated that the operational bandwidth for 5G is expected to be between 3.4 and 3.6 GHz.

**VI. EFFECTS OF USER'S ON 5G MOBILE TERMINAL ANTENNAS**

The upcoming 5G technology launch by 2020 is also capitalized by developers for active array systems and chipset manufacturers to meet the needs for complete deployment [84]. The frequency band lower than 6 GHz known as sub-6 GHz

5G band for mobile terminal antenna is band of interest for many countries. The antenna design for mobile terminals must also account for the effects of its housing and location of the radiator for optimized MIMO performance [85]. While the interaction of terminal with the user's hand for GSM, LTE, WLAN, WiMAX and another cellular band below 3.5 GHz mobile terminals have been investigated in previous literature [86], there is a need for such research in the 5G bands. Such research are still limited, especially for antennas operating in the vicinity of the 5G sub-6GHz band [87]–[91]. One of such research is a 12-port 5G massive MIMO antenna array in the sub-6GHz for mobile terminals investigated considering the user's hand [87]. However, the placement of the user's hand seen in [87] is inaccurate, with the hand inserted inside the chassis of the mobile terminal. The hand is also placed opposite the antenna, at locations where there is no direct interaction with the antenna's radiating areas with more than 50 % of radiated power. Meanwhile, a study in terms of specific absorption rate is presented in [88], performed on a two-element quad band antenna array placed on different locations on the chassis. It was concluded that the SAR values for the antenna located at the bottom of the chassis resulted in lower SAR due to the larger distance of this antenna from the human head. Next, a simple study of the index finger's influence on a PIFA antenna performance is discussed in [89]. The effect of a user's finger is studied on sixteen finger locations, indicating

TABLE 7. Summary for 5G mobile terminal antennas with user’s influence [87]–[91].

Ref	Antenna Design	Bandwidth [GHz]	Ref	Antenna Design	Bandwidth [GHz]
[87]		3.4 - 3.8 and 5.15 - 5.925	[90]		3.4 - 3.6
[88]		1.565 - 1.585, 2.4 - 2.484, 2.5 - 2.57, 2.62 - 2.69, 3.3 - 3.4 and 5.15 - 5.35	[91]		5.0 - 6.0
[89]		4.5 - 5.5			

radiation losses and matching efficiency of up to  $-1.6$  dB and  $-0.9$  dB, respectively, in the 5 GHz band. Finally, the user’s effect on a mobile terminal phased array was investigated in [90] and [91]. In [90] it was observed that the phased array antenna designed on the metal frame used in data mode suffered losses of up to 3 dB, a loss of at least 5 dB is observed at 3.5 GHz band when two hands is used to hold the terminal. The users’ effects are also investigated further up the frequency, from 5 to 6 GHz, and is presented in [91]. It is shown that the operation of the antenna in the mobile terminal is degraded in terms of gain by up to 2 dB and 7 dB, when used near a user’s hand and head, respectively.

Due to the limited available research in the 5G sub 6 GHz band, it is difficult to conclude accurately how the user’s effects may affect antenna parameters. It is known that the user’s hand affects the antenna performance differently when the operated in the lower (below 3 GHz) and higher (above 3 GHz) frequencies. This is a cause for concern as the two main frequencies expected to be used for the 5G sub-6 GHz band are from 3.4 to 3.6 GHz (Band C) and from 5.15 to 5.925 GHz (LTE-U band 46).

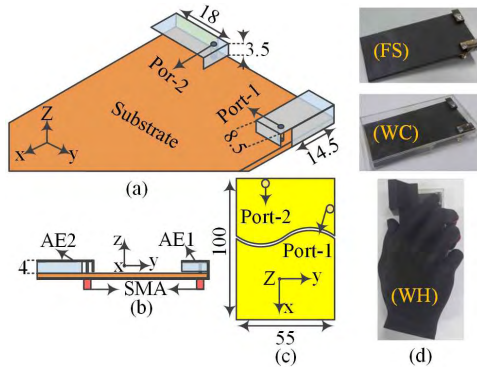
**VII. EFFECTS OF USER’S HAND ON 5G SUB-6GHZ BANDS**

The detailed review of mobile terminal antennas provided in the previous sections indicated that there is a need for new antennas operational within the sub-6 GHz 5G frequencies

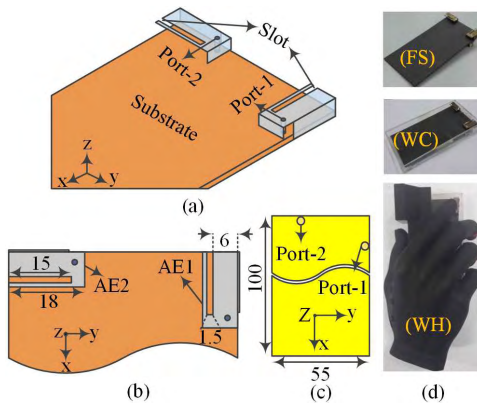
besides supporting existing mobile frequencies. This work is attempted to investigate the effects of the user’s hand in two sub-6 GHz 5G bands. In this work, two antennas were designed: the first is operational in LTE band 46 (AD1), whereas the second, is a dual band antenna operating in the Band C as its lower band (LB) and LTE Band 46 as its upper band (UB) (denoted as AD2). They are both placed orthogonally on a same mobile terminal chassis before their performance are being investigated in free space and in proximity of two hand phantoms.

**A. WIDEBAND (AD1) AND DUAL BAND (AD2) MOBILE TERMINAL ANTENNA**

The detailed dimensions for AD1 and AD2 are illustrated in Figure and Figure 2. The two identical PIFAs are placed orthogonally relative to each other on the edges of a 1.575 thick Rogers RT/Duroid-5880 substrate with a surface area of  $55 \times 110 \text{ mm}^2$  for both AD1 and AD2, see Figure 3(a). This is to maximize isolation between them. The dielectric permittivity of the substrate is 2.2 and its loss tangent is 0.0009. The copper metallization on the substrate is 0.035 mm thick (i.e., yellow region in Figures 2 and 3) on its reverse side. The copper plate forming the PIFA element is 0.291 mm thick. Each PIFA is fed using a  $50 \Omega$  coaxial probe, at an optimized location. To fine tune impedance bandwidth, a 3.5 mm folded extension is introduced at the top edge of



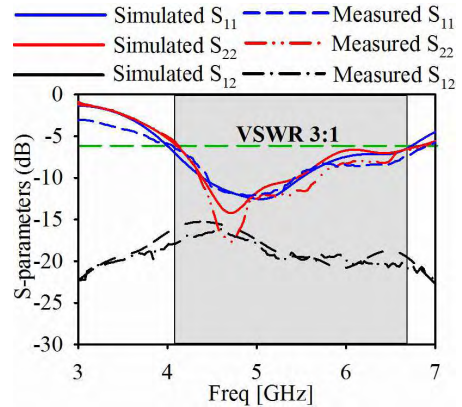
**FIGURE 2.** Geometry of the proposed AD1, in (a) 3D view, (b) side view, (c) bottom view and (d) prototype in free space (FS), with casing (WC), and with hand (WH).



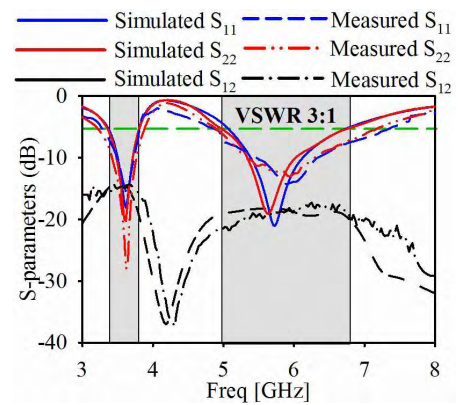
**FIGURE 3.** Geometry of proposed (AD2), in (a) 3D view, (b) top view, (c) bottom view and (d) prototype in free space (FS), with casing (WC), and with hand (WH).

between two resonant lengths in the top plate (See Figure 3). Upon optimization of AD1 and AD2, both antennas are fabricated as shown in Figures 2(d) (for AD1) and Figures 3(d) (for AD2). Different from AD1, a slot is etched onto each antenna element for AD2 to facilitate the separation of two bands. The simulated and measured S-parameters for the proposed AD1 MIMO antenna presented in Figure 4 indicate good agreements. The measured  $-6$ dB impedance bandwidth is 2.68GHz (from 4 to 6.68GHz) for antenna element 1 (AE1) and 2.82GHz (from 3.92 to 6.74GHz) for antenna element 2 (AE2). This fulfills the frequency band requirement for LTE Band 46. The isolation within the 2.68 GHz and 2.82GHz band is between 16dB and 21dB. On the other hand, a comparison between the measured and simulated S-parameters for AD2 is shown in Figure 5.

Measurements indicate that AD2 operates from 3.35 to 3.59 GHz (in the C Band) and from 5.15 to 6.8 GHz which fulfills the requirement of LTE Band 46 (with at least  $-6$  dB of reflection coefficient). Within the operational bands, the isolation is  $-15$  dB and  $-18$  dB in the lower band and upper band, respectively. In general, the simulated and measured results agreed well, with minor discrepancies caused by fabrication inaccuracies.



**FIGURE 4.** Simulated and measured S-parameters in free space for AD1.



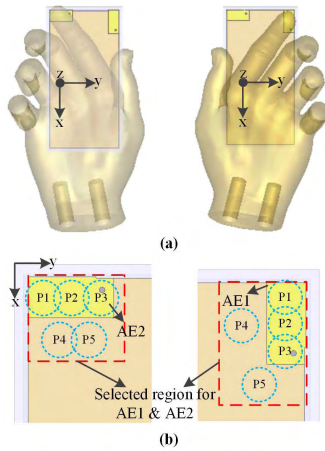
**FIGURE 5.** Simulated and measured S-parameters in free space for AD2.

**B. USER'S IMPACT ON THE PERFORMANCE OF AD1**

Since AD1 operates well throughout the whole frequency range for LTE Band 46, the effects of the user's hands on the antenna's impedance matching (IM), mutual coupling (MC) and radiation efficiency (RE) are evaluated next. This study is setup by inserting the antenna prototype into a 1 mm thick casing dimensioned at  $112 \times 57 \times 7.7$  mm<sup>3</sup>; see Figure 2(d)). This casing is made using poly (methyl methacrylate) with a permittivity,  $\epsilon_r$  of 2.8. For a realistic representation of mobile terminal casings in practice, and to emulate the worst-case interaction, the antenna is positioned within the box to achieve a minimal separation of 1 mm to the user's finger. Figure 6(a) illustrates simulation of AD1 with the bounding box and the right hand (RH) and left hand (LH) of a SHO3TO6-V3 phantom [12] (with  $\epsilon_r = 22.5$  between 3 and 6 GHz). Both user hands were accounted for during performance evaluations due to the orthogonal placement of the AEs on the PCB. When holding a mobile phone, the closest user's component to the AEs is the finger, thus it is imperative that their interactions with the radiated waves be characterized.

The index finger is positioned at five different locations (P1, P2, P3, P4, and P5) in the vicinity of the AEs, as illustrated in Figure 6(b), while keeping the hand position constant. P1, P2 and P3 are located on top of the radiating





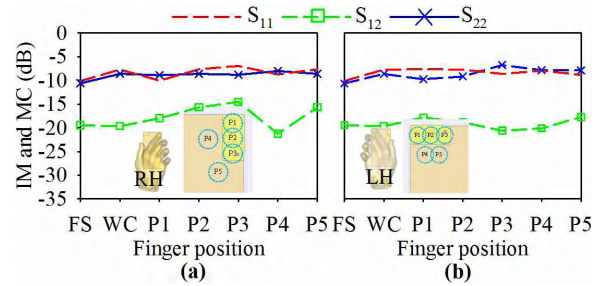
**FIGURE 6.** Simulation of AD1 with user's (a) LH and RH, and (b) index finger positions for analysis of user effect.

element, whereas P4 and P5 are positioned on the bottom and side of the AEs, respectively. Since most of the antenna radiation originates from the top surface, P1, P2 and P3 are locations representing direct interference by the finger on the AEs. On the contrary, P4 and P5 are finger locations which are non-directly interfering with the antenna. Evaluation for all locations in this study is performed using the center frequency of AD1 at 5.41 GHz. This choice of the center frequency is expected to be most representative of its performance throughout the entire operating bandwidth. Moreover, for evaluations with users using the phantom, evaluation at the center frequency also ensure that the simulations are performed using the most average properties of the user's hand throughout the operating frequency band, which is most reasonable, especially when the operating bandwidth is large.

**1) USER'S IMPACT ON IM AND MC**

First, the effects of the user's right and left hands on the IM, MC, and bandwidth with different index finger locations near the AEs are simulated, see Figure 7. The following observations can be made.

- The impedance matching of the AD1 in free space (FS) is  $-11$  dB at its center frequency. The positioning of hand as well as with casing (WC) decreases the IM of antenna by up to 4 dB due to the dielectric properties of the casing and the user's hand.
- In all studied cases, the index finger placed at positions P1, P2 and P3 affected all assessed parameters more significantly compared to P4 and P5 due to the fingers' location in the way of the antenna's radiation. This is validated by observing the worst IM, which is when the finger is placed on P3, i.e. on top of the highly radiative area of the antenna. In Figure 2 it can be seen that antenna patch is directly fed by a coaxial probe. It is generally observed that the current distribution changes as the finger placement is varied on top of the antenna.



**FIGURE 7.** Effect on AD1 MIMO showing (a) effect of RH on AE1 IM and MC, and (b) effect of LH on AE2 IM and MC.

This then affected the antenna performance in terms of IM, and is worst when the finger is placed at the coaxial probe feed (P3), where the current is highest. This is mainly due to the finger's more significant interaction with the antenna's impedance at this high current position (P3) as compared to the other two (P1 and P2) positions.

- When the hand is closely located to the AEs, the MC varied differently for both AEs for all selected locations: up to 4 dB when the antenna is held in the right hand and 6 dB in the left hand, see Figure 7.
- Impedance bandwidth variation is also observed. This is due to the lengthening of the electrical length of the chassis due to the dielectric loading by the casing and phantom. Table 7 summarizes the impedance bandwidth for both AEs at different locations.

**2) USER'S IMPACT ON RE**

Firstly, the RE of the antenna are simulated in FS and WC (see Figure 8) to obtain their reference efficiency. These values are then compared with the RE of the antennas evaluated in the vicinity of the SHO3TO6-V3 left and right-hand phantoms, as illustrated in Figure 8(a) and (b). These results indicate that the hands decrease the RE at least by 2.5 dB, and up to 4.8 dB in the worst case when held in the RH, relative to the RE in free space. Similarly, the RE for the antenna when held in the LH is observed as 3 dB, and in worst case up to 5.8 dB. It is clear from the figures that P1, P2 and P3 significantly affects the RE of both antenna elements, especially when located at P2 and P3, when the index figure is placed exactly or near to the feed point of the antenna. Besides the fact being radiating through that particular region, the high radiation quality factor of the AEs lead to relatively high resistive losses compared to the structures with lower radiation.

**C. EXPERIMENTAL ASSESSMENT OF AD1**

The fabricated prototype of the proposed AD1 is presented in Figure 2(d). Simulated and measured S-parameters, efficiency and MIMO performance parameters (envelop correlation coefficient (ECC) and multiplexing efficiency (ME))



TABLE 8. Simulated Bandwidth for the wideband MIMO antenna (AD1) with right and left hand.

	Bandwidth	FS	WC	P1	P2	P3	P4	P5
		[GHz]	[GHz]	[GHz]	[GHz]	[GHz]	[GHz]	[GHz]
RH	AE1	(3.92 -6.74)	(3.70 -6.515)	(3.82 -6.73)	(3.62 -6.40)	(3.62 -6.43)	(3.88 -6.89)	(3.76 -7.10)
	AE2	(4.06 -6.70)	(3.79 -6.62)	(3.95 -6.73)	(3.90 -6.91)	(3.87 -6.60)	(3.88 -6.89)	(3.76 -7.10)
LH	AE1	(3.92 -6.74)	(3.70 -6.515)	(3.92 -6.57)	(3.94 -6.46)	(3.95 -6.43)	(3.90 -6.49)	(3.88 -6.50)
	AE2	(4.06 -6.70)	(3.79 -6.62)	(3.67 -7.01)	(3.69 -7.15)	(3.69 -5.78)	(3.75 -6.96)	(3.85 -6.84)

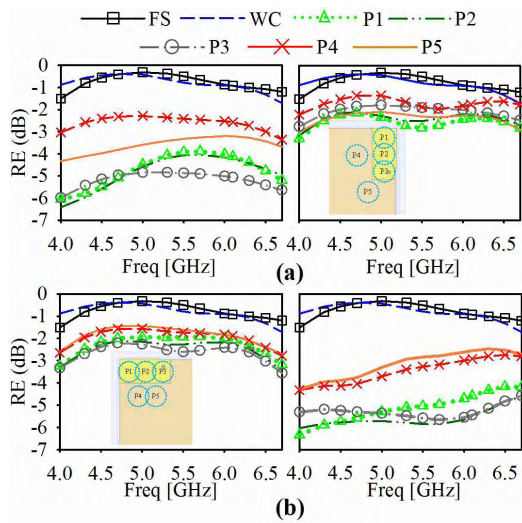


FIGURE 8. Effect on AD1 MIMO showing (a) effect of RH on RE (left) AE1 and (right) AE2 and (b) effect of LH on RE (left) AE1 and (right) AE2.

when placed in the casing and held in user’s hands are shown in Figures 9 and 10. These figures indicate good simulation-measurement agreements. The measured reflection coefficient ( $S_{11}$ ) of AD1 with casing resulted in a 6dB bandwidth of 2.81 GHz (from 3.70 to 6.515 GHz) with a downward shift of 220 MHz compared to in FS. For the case held in user’s hand, the measured S-parameter shown in Figure 9(b) indicates a downwards shift of 300 MHz, with about 4 dB of additional impedance mismatch relative to FS. The impedance mismatch and shift in resonant frequency is due to dielectric loading of casing and user’s hand on the mobile terminal. The original operating bands of AD1 are shaded in Figure 9(a) and (b) to facilitate the identification of the resonance shift.

The RE of the antennas is then measured with one antenna excited while the other antenna ports are terminated using a 50  $\Omega$  load before every evaluation. Figure 10(a) and (b) shows the simulated and measured antenna RE in FS, WC, and with user (WU), indicating a maximum RE of  $-0.8$  dB for both AEs in FS and WC. Meanwhile, up to 4.5 dB of

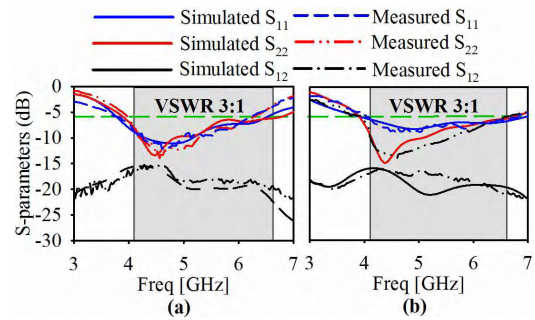
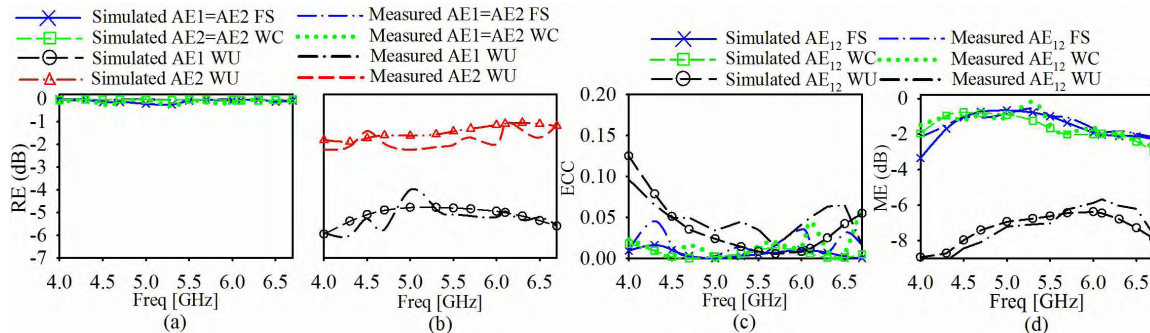


FIGURE 9. Simulated and measured S-parameters of AD1 (a) WC and (b) WU.

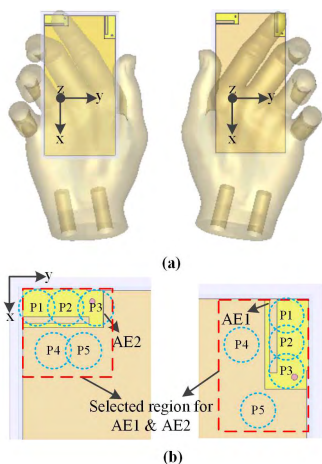
loss can be observed from Figure 10(b) when the antenna is in close proximity to the user. Figure 10(c) shows the measured ECC of all scenarios (FS, WC, and WU) and it is seen that the ECC in all cases is not significantly affected. Thus, this evaluation is extended to study ME, as illustrated in Figure 10(d) in all scenarios. Notice that the losses in terms of ME is around 5 dB in WU compared to the cases in FS or WC. Figure 10(c) shows the presence of user hand increases the ECC between ports. However, even when in the presence of the user’s hand, the correlations between the ports are still low, with a maximum measured ECC value of 0.12 at 4 GHz. This evaluation is then extended to study ME in all scenarios, as illustrated in Figure 10(d). Notice that the losses in terms of ME is quantified to be about 5 dB in WU compared to the cases in FS or WC, which is caused by the differences in radiation efficiencies in the presence of user’s hand. The antenna with degraded total efficiency caused reduction in the signal-to-noise (SNR) of the received signals, and consequently affected ME, as this parameter is dependent on both the ECC and total efficiency [92].

D. USER IMPACT ON THE PERFORMANCE OF AD2

Next, AD2 is assessed in the presence of the same hand phantoms as was performed for AD1. Due to their same sizes, AD2 can be fairly compared to AD1 in terms of IM, MC, RE. The same casing is also used for AD2 as discussed before,



**FIGURE 10.** Simulated and measured results for AD1 (a) RE in FS and WC, (b) RE in WU scenario, (c) ECC in all scenarios (FS, WC and WU) and (d) ME in all scenarios (FS, WC and WU).

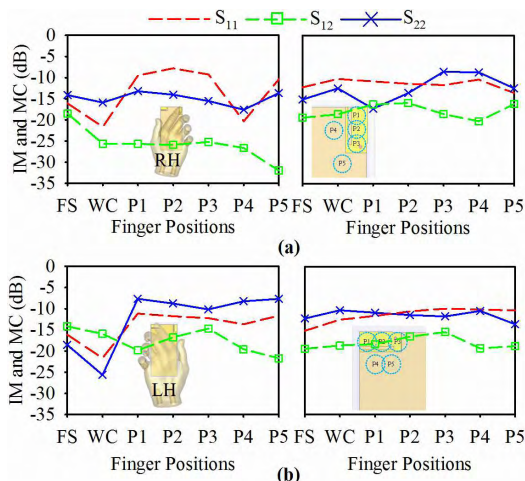


**FIGURE 11.** Simulation setup of AD2 with user's (a) LH and RH and (b) index finger positions.

and its evaluation setup with SHO3TO6-V3 left and right hands is illustrated in Figure 11(a). Similarly, five different locations of index finger are chosen (P1, P2, P3, P4, and P5) placed in the radiating elements, see Figure 11(b). Evaluations are mainly performed at the center frequency of the LB (3.58 GHz) and UB (5.885 GHz) for this dual band MIMO antenna.

1) USER'S IMPACT ON IM AND MC

Due to the contribution of the slot in enabling the additional resonance in AD2, it is important to account its behavior when placed in vicinity of user. To ensure consistency, the palm-to-handset gap is being kept constant as during evaluations for AD2. Figure 12 illustrates the IM and MC for user's LH and RH at five different index finger locations (P1, P2, P3, P4, and P5). The IM in free space for LB and UB is -16 dB, whereas the IM variation in presence of user hand for AE1 is observed up to 8 dB for LB and 4 dB in the UB for the RH phantom. Similarly, for AE2, 4 dB variations are observed in both LB and UB with user's LH, see Figure 12(b). The MC is also evaluated for the dual band case in all five locations. Due to the orthogonal placement of the two AEs,



**FIGURE 12.** User effects on AD2: (a) effect of RH on AE1 IM and MC, (left) LB and (right) HB and (b) effect of LH on AE2 IM and MC, (left) LB and (right) HB.

the resulting MC caused by the LH and RH are slightly different: with about 4 dB of variation when held using the LH and 2 dB for RH, depending further on the location of user's finger around AEs. Upon evaluation of IM and MC, the impedance bandwidth changes in both bands for all index finger locations is studied, and is summarized in Table-8.

2) USER'S IMPACT ON RE

Figure 13 illustrates the effects of the finger placement on RE with casing, relative to its performance in FS. This is followed by studying the effects of the user's hand on RE. As expected, lower values of RE are obtained when a hand is present in the vicinity of AD2, especially when index finger is positioned right on top of the antennas (P1, P2 and P3). RE starts decreasing up to 4.6 dB and 5.2 in the LB and UB, respectively, in the presence of the LH. Likewise, RE in LB and UB varies between 4 dB and 6 dB, respectively for RH. It is shown from Figure 12 that the most sensitive part of proposed AD2 for RE is when finger is closest to the most radiative part of the antenna (P2 and P3). Besides the decrease in RE, these locations also resulted in degradation of

TABLE 9. Simulated bandwidth for dual band MIMO antenna (AD2) with right and left hand.

	Bandwidth	Band	FS [GHz]	WC [GHz]	P1 [GHz]	P2 [GHz]	P3 [GHz]	P4 [GHz]	P5 [GHz]
	RH	AE1	LB	(3.38 -3.78)	(3.28 -3.68)	(3.25 -3.67)	(3.24 -3.65)	(3.16 -3.74)	(3.22 -3.77)
HB			(5.15 -6.62)	(5.00 -6.48)	(5.02 -6.57)	(5.17 -6.87)	(5.05 -6.98)	(4.99 -6.85)	(5.26 -6.93)
AE2		LB	(3.39 -3.78)	(3.33 -3.77)	(3.36 -3.80)	(3.36 -3.79)	(3.35 -3.77)	(3.34 -3.77)	(3.33 -3.77)
		HB	(5.05 -6.62)	(4.97 -6.72)	(4.95 -6.69)	(4.93 -6.70)	(4.95 -6.68)	(4.97 -6.81)	(5.03 -6.65)
LH	AE1	LB	(3.38 -3.78)	(3.34 -3.76)	(3.26 -3.63)	(3.26 -3.63)	(3.25 -3.63)	(3.26 -3.63)	(3.27 -3.62)
		HB	(5.15 -6.62)	(5.00 -6.48)	(4.91 -6.44)	(4.91 -6.3)	(4.89 -6.32)	(4.79 -6.43)	(4.79 -6.45)
	AE2	LB	(3.39 -3.78)	(3.33 -3.77)	(3.23 -3.68)	(3.23 -3.67)	(3.19 -3.68)	(3.17 -3.63)	(3.15 -3.62)
		HB	(5.05 -6.62)	(4.97 -6.72)	(4.98 -7.00)	(4.97 -7.15)	(4.7 -6.89)	(4.94 -6.86)	(4.93 -6.78)

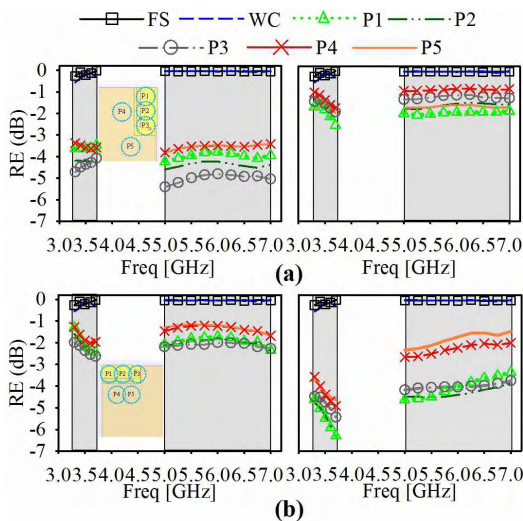


FIGURE 13. User’s effect on AD2: (a) effect of RH on RE (left) AE1 and (right) AE2 and (b) effect of LH on RE (left) AE1 and (right) AE2.

the impedance matching. It is concluded that the user’s hand affected AD2 differently for the two AEs, where AE2 exhibit less loss in RE as compared to AE1.

E. EXPERIMENTAL ASSESSMENT OF AD2

The proposed AD2 is then fabricated and tested, as shown in Figure 3(d), and its feeding points are kept same as AD1. The measured S-parameters in both WC and WU scenarios are shown in Figure 14, indicating a reasonable agreement with simulations. A downward shift of 100 MHz in the LB and 150 MHz in the UB are observed due to the dielectric loading of the casing. Meanwhile, 140 MHz of downwards

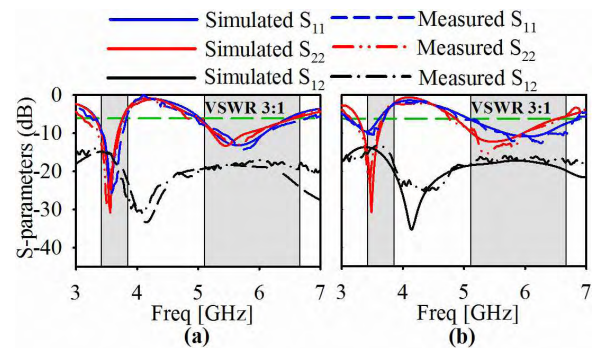
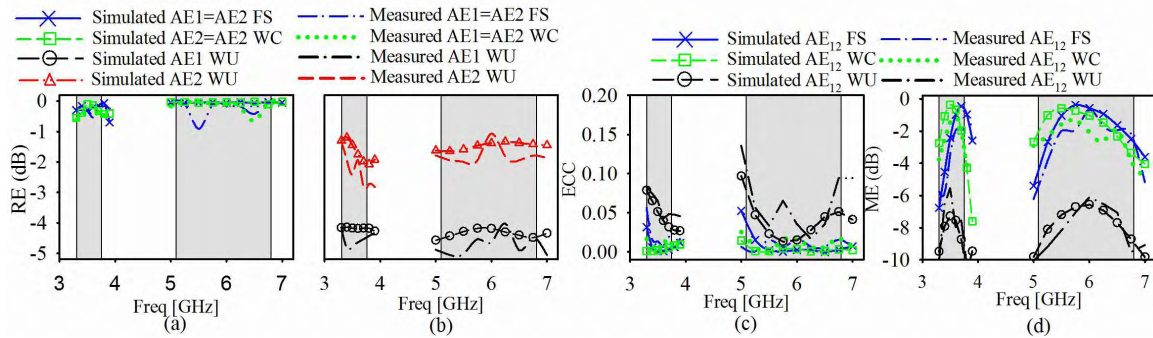


FIGURE 14. Simulated and measured S-parameters of AD2: (a) with casing and (b) with user’s hand.

shifting in the LB and 220 MHz in the UB are observed for AE1 in proximity of a user’s hand. The measured bandwidth with casing is from 3.44 to 3.99 GHz (in the LB) and from 5.00 to 6.725 GHz (in the UB). On the other hand, the most affected element for AD2 is AE1 due to the location of the index finger placed directly over it. The antenna bandwidth then changes to be from 3.120 to 3.62 GHz (in the LB) and from 4.889 to 6.624 GHz (in the UB), with simultaneous impedance mismatch of 11 dB and 4 dB in the LB and UB, respectively.

The antenna RE for AD2 is also measured in sequence for all scenarios (FS, WC and WU), with the adjacent (not assessed) antenna terminated using a 50 Ω load. The measured RE in the C band and LTE Band 46 varied approximated between 4.6 dB and 5.2 dB in the LB and UB, respectively, see Figure 15. Measured ECC is then calculated to assess the MIMO performance of AD2 using 3D field radiation patterns,





**FIGURE 15.** Simulated and measured results for AD2 (a) RE in FS and WC, (b) RE in WU scenario, (c) ECC in all scenarios (FS, WC and WU) and (d) ME in all scenarios (FS, WC and WU).

assuming a uniform 3D angular power spectrum. The ECC in Figure 15(c) is less than 0.08 and 0.12 in the LB and UB, respectively. This indicates satisfactory MIMO performance for both operating bands of AD2. From Figure 15(d), it is also observed that the ME of AD2 is also affected by the presence of the user's hand, with losses of around 4 dB and 3.5 dB in the LB and UB, respectively, relative to FS. This is intuitive as antenna with degraded efficiency will reduce signal-to-noise ratio of the received signal

## VIII. CONCLUSION

In this paper, single and MIMO terminal antennas for current future 5G wireless communication bands considering user's interaction have been reviewed. It is shown that the evolution of the spectrums of mobile technologies towards 5G have mainly influenced antennas' operational requirements, and consequently their development trends, from functioning in a single band to multiband, followed by MIMO to massive MIMO. In this context, this review aims to provide, discuss and summarize researches relevant to the design and alleviation of users' effects on current mobile antennas in the design process. Recent investigations on mobile terminal antennas for different dual-, multi- and wideband characteristic indicate that the implementation of different broadbanding and multibanding techniques are needed to meet the more challenging hardware requirements. It also imperative for mobile terminal antennas to be built in their casings, and designed to be more compact in size to meet the demands of multi-wireless standards operation using a single device. The findings of this review can be categorized into three major aspects.

### A. LITERATURE SURVEY OF MIMO MOBILE TERMINAL ANTENNAS

Recent MIMO terminal antennas for different frequencies, including different decoupling techniques are presented and discussed. They include concept of neutralization line, use of parasitic element, ground perturbations, decoupling slot line, orthogonal polarization, a T-shaped transformer and the use of metamaterials. The choice of the different techniques used for MIMO antenna decoupling is mainly dependent on the

operating frequency bands. It is also observed that a neutralizing line is useful when the antenna is operating in a single band, whereas a T-shaped transformer and ground current modification facilitate decoupling for dual band antennas. Finally, multiband antennas are most effectively decoupled using ground perturbation and decoupling slots lines. The newly defined MIMO antenna multiplexing efficiency was also described, showing the relation between the MIMO performance parameters and efficiencies versus the correlation of the antenna elements for 5G bands.

The future focus of mobile terminal antenna is to utilize the 5G frequency bands along with other cellular bands. As the 5G technology is maturing, research efforts are being intensified in many countries. Due to this factor, several different frequencies have been investigated for 5G mobile terminal, which includes the band from 2.5 to 2.65 GHz, from 3.58 to 4 GHz and from 4.98 to 6.01 GHz. Nonetheless, it is noticed that most researched band below 6 GHz is focused in the bands between 3.4 and 3.6 GHz, and from 5.15 to 5.925 GHz. This indicates that the operational bandwidth for 5G is expected to be either one of these two bands, and these bands can be categorized as the sub-6 GHz 5G bands.

### B. ANALYSIS OF USER'S HAND ON 5G MOBILE TERMINAL ANTENNAS

However, antennas for terminals must also account for the effects of users' proximity during operation. Due to the different characteristic of user's skin properties at frequencies above 3 GHz and the limited available research on this aspect, it is difficult to accurately predict the effects of user's hand on antenna parameters by examining previous research on lower frequency bands. To fulfill this research gap, several antennas have been designed and investigated with the influence of users for wide and dual band sub 6GHz frequencies in this work. The two antennas, AD1 and AD2, are sized similarly, fed using the same connectors and built using the same materials. AD1 is designed for wideband operation in LTE Band 46, whereas AD2 is designed to operate in dual band mode in the C band and LTE Band 46. Evaluations in proximity of user's hand are performed using the right and left-hand phantoms, both in simulations and

measurements. This is to examine the changes in terms of IM, MC and impedance bandwidth, RE, ECC and ME. From the simulations and measurements, it is observed that the presence of the hand affected the matching more significantly in AD2 compared to AD1, especially in the LB. This is due to strong current distribution around the slot in AD2, which is critical in splitting the wideband operation into two to enable the dual band operation of AD2. The change in terms of impedance matching when the user's finger is placed on a high current area near to the slot indicates its sensitivity as the LB operation requires a longer electrical length. Nonetheless, the detuning of the impedance bandwidth for both antennas indicated consistency as they are both generally shifted downwards due to the dielectric loading of the casing and hand. Moreover, variation of MC between the two antenna elements is constant, besides the consistent decrease of the RE. Placement of the user's hand directly on top of the antenna element (at locations P1, P2 and P3) influenced their performance significantly. On the contrary, locating the hand at a distance from the antenna elements can in some cases even improve the MC of the antennas. This is due to the radiated power being coupled to the user's index finger, which means that the smaller E-field strength results in less MC in the presence of the hand in comparison to the free space. Besides that, other antenna parameter remains unaffected. The finding from this investigation provides a good understanding on the effects of user's hands in designing future 5G mobile terminals in the sub-6 GHz band.

### C. FUTURE STRATEGIES TO IMPROVE MIMO MOBILE TERMINAL ANTENNAS

Several practical issues on how the human body impacts the antenna operation and efficiency were studied using single and multi-element antennas, besides reviewing the related recent and ongoing researches. Due to its small size requirements, the need of the integration of multiband and multi-wireless standard using a single hardware and mitigating the human body effects, antenna design for mobile phone is always the art of compromising between the size, the phone appearance, and the performance.

Smartphones with full metal casing is also gaining significant interest in recent years in the mobile phone industry. This is due to their improved mechanical strength, attractive appearance, and better thermal conductivity. A number of such designs have been proposed, especially for frequencies below 3 GHz, but there is no study reporting the reduction in performance due to the effects of user's thus far. This is possibly another research aspect which is of interest for future investigations, especially methods in overcoming performance variations and the effects of users due to the use of continuous metal rims in smartphone antennas. Upcoming researches are foreseen to be focused on the optimization of the performance-enhanced multiband and reconfigurable multi-antenna and massive MIMO systems for future wireless generations, with the aim of reducing the impact of the human body.

### REFERENCES

- [1] S. Zhang, K. Zhao, Z. Ying, and S. He, "Body-effect-adaptive compact wideband LTE MIMO antenna array with quad elements for mobile terminals," in *Proc. PIERS*, vol. 1, 2013, pp. 1858–1861.
- [2] S. Zhang and Z. Ying, "MIMO antennas for mobile terminals," in *Proc. FERMAT*, 2016, pp. 725–727.
- [3] Z. Ying, "Antennas in cellular phones for mobile communications," *Proc. IEEE*, vol. 100, no. 7, pp. 2286–2296, Jul. 2012.
- [4] Z. N. Chen, D. X. Liu, H. Nakano, X. M. Qing, and T. Zwick, *Handbook of Antenna Technologies*. Singapore: Springer, vol. 2, 2016, pp. 1409–1411.
- [5] R. Valkonen, J. Ilvonen, C. Icheln, and P. Vainikainen, "Inherently non-resonant multi-band mobile terminal antenna," *Electron. Lett.*, vol. 49, no. 1, pp. 11–13, Jan. 2013.
- [6] A. Cihangir, F. Ferrero, G. Jacquemod, P. Brachat, and C. Luxey, "Integration of resonant and non-resonant antennas for coverage of 4G LTE bands in handheld terminals," *Forum Electromagn. Res. Methods Appl. Technol.*, vol. 3, no. 5, pp. 1–12, 2014.
- [7] WRC-15 Press Release. *World Radio Communication Conference Allocates Spectrum for Future Innovation*. Accessed: 2015. [Online]. Available: [http://www.itu.int/net/pressoffice/press\\_releases/2015/56.aspx](http://www.itu.int/net/pressoffice/press_releases/2015/56.aspx)
- [8] *4G Americas, White paper on 5G Spectrum Recommendations*. [Online]. Available: [http://www.5gamericas.org/files/6514/3930/9262/4G\\_Americas\\_5G\\_Spectrum\\_Recommendations\\_White\\_Paper.pdf](http://www.5gamericas.org/files/6514/3930/9262/4G_Americas_5G_Spectrum_Recommendations_White_Paper.pdf)
- [9] MT-2020 (5G) Promotion Group. (2015). *White Paper on 5G Concept*. [Online]. Available: <http://www.imt-020.org/cn/zh/documents/download/4>
- [10] *China Reserves Spectrum for 5G Services*. Accessed: Nov. 2017. [Online]. Available: <http://www.atimes.com/article/china-reserves-spectrum-5g-services/>
- [11] Qualcomm. (2015). *Making the Best Use of Licensed and Unlicensed Spectrum*. [Online]. Available: <https://www.qualcomm.com/media/documents/files/making-the-best-use-of-unlicensed-spectrum-presentation.pdf>
- [12] SK Telecom. (2015). *SK Telecom 5G White Paper*. [Online]. Available: <http://www.sktelecom.com/img/pds/press/SKT-5G%20White%20Paper-V1.0-Eng.pdf>
- [13] (2016). *Speag*. [Online]. Available: <https://www.speag.com/products/emphantom/hands/3to6ghz-hands-2>
- [14] M. Kim, W. Lee, and Y. J. Yoon, "Wideband antenna for mobile terminals using a coupled feeding structure," in *Proc. IEEE Int. Symp. Antennas Propag.*, Jul. 2011, pp. 1910–1913.
- [15] Z. Lin, H. Liu, and C. Liu, "Design of sleeve broadband antenna for mobile terminals," in *Proc. Prog. Electromagn. Res. Symp. (PIERS)*, Aug. 2016, pp. 487–490.
- [16] R. Rahman, K. M. Morshed, S. Sabrin, and M. Rahman, "Wideband planar monopole antenna for LTE, GSM, Bluetooth, WiMAX, DCS, PCS, and GPS mobile terminals," in *Proc. 2nd Int. Conf. Elect. Inf. Commun. Technol. (EICT)*, Dec. 2015, pp. 309–313.
- [17] R. Gómez-Villanueva, H. Jardón-Aguilar, and R. Linares-Y-Miranda, "Broadband PIFA antenna for mobile communications terminals," in *Proc. 11th Int. Conf. Elect. Eng. Comput. Sci. Autom. Control (CCE)*, Sep./Oct. 2014, pp. 1–6.
- [18] J. Holopainen, J. Ilvonen, R. Valkonen, A. A. H. Azremi, and P. Vainikainen, "Study on the minimum required size of the low-band cellular antenna in variable-sized mobile terminals," in *Proc. 6th Eur. Conf. Antennas Propag. (EuCAP)*, Mar. 2012, pp. 2754–2758.
- [19] R. Islam and M. Ali, "Ground current modification of mobile terminal antennas and its effects," *IEEE Antennas Wireless Propag. Lett.*, vol. 10, pp. 438–441, 2011.
- [20] K. Wang, R. A. M. Mauer Mayer, and T. F. Eibert, "Contour-integrated dual-band compact antenna elements and arrays for low-profile mobile terminals," *IEEE Trans. Antennas Propag.*, vol. 63, no. 7, pp. 3305–3311, Jul. 2015.
- [21] J. Ahn, S. Kim, M.-J. Lee, and Y.-S. Kim, "A compact printed dual-band WLAN antenna with a shorted coupling strip for mobile terminals," in *Proc. Asia-Pacific Microw. Conf. (APMC)*, Dec. 2012, pp. 313–315.
- [22] J.-H. Kim, Y.-B. Chae, J.-H. Lim, and T.-Y. Yun, "Printed internal antenna for mobile broadcasting (DVB-H/T-DMB) and communications (GSM900)," *IET Microw., Antennas Propag.*, vol. 6, no. 6, pp. 680–684, Apr. 2012.
- [23] L. Li, Z. Jia, F. Huo, and W. Han, "A novel compact multiband antenna employing dual-band CRLH-TL for smart mobile phone application," *IEEE Antennas Wireless Propag. Lett.*, vol. 12, pp. 1688–1691, 2013.



- [24] Y. Du and A. Zhao, "An internal quad-band printed monopole antenna for oval-shaped mobile terminals," *IEEE Trans. Magn.*, vol. 48, no. 2, pp. 683–686, Feb. 2012.
- [25] J. Guo, L. Zhou, B. Sun, and Y. Zou, "Magneto-electric monopole antenna for terminal multiband applications," *Electron. Lett.*, vol. 48, no. 20, pp. 1249–1250, Sep. 2012.
- [26] K.-C. Lin, C.-H. Lin, and Y.-C. Lin, "Simple printed multiband antenna with novel parasitic-element design for multistandard mobile phone applications," *IEEE Trans. Antennas Propag.*, vol. 61, no. 1, pp. 488–491, Jan. 2013.
- [27] I. Ahmed, I. Shoaib, N. Shoaib, A. Rasheed, and S. Shoaib, "A printed hybrid loop planar inverted-f antenna for next generation handheld terminals," in *Proc. Eur. Conf. Antennas Propag. (EuCAP)*, Apr. 2013, pp. 2044–2047.
- [28] T.-N. Mai, A.-C. Lepage, B. Huyart, and Y. Pinto, "Compact multi-band planar monopole antenna for LTE terminals," in *Proc. 8th Eur. Conf. Antennas Propag. (EuCAP)*, Apr. 2014, pp. 3278–3280.
- [29] M. Ur-Rehman and S. Haxha, "Design of a slotted-patch microstrip antenna for mobile terminals," in *Proc. IEEE Int. Symp. Antennas Propag. USNC/URSI Nat. Radio Sci. Meeting*, Jul. 2015, pp. 1716–1717.
- [30] W. Chen, Y. Yao, J. Yu, X. Liu, and X. Chen, "Design of a novel multi-band antenna for mobile terminals," in *Proc. Int. Wireless Symp. (IWS)*, Mar./Apr. 2015, pp. 1–4.
- [31] Y. Guo, H. Liu, X. Dai, and Z. Lin, "Design of multi-band antenna for 4G mobile terminals," in *Proc. Progr. Electromagn. Res. Symp. (PIERS)*, Aug. 2016, pp. 491–493.
- [32] M. Sonkki, E. Antonino-Daviu, M. Ferrando-Bataller, and E. T. Salonen, "Planar wideband polarization diversity antenna for mobile terminals," *IEEE Antennas Wireless Propag. Lett.*, vol. 10, pp. 939–942, 2011.
- [33] G. Kang, Z. Du, and K. Gong, "Compact broadband printed slot-monopole-hybrid diversity antenna for mobile terminals," *IEEE Antennas Wireless Propag. Lett.*, vol. 10, pp. 159–162, 2011.
- [34] M. Sonkki, E. Antonino-Daviu, M. Cabedo-Fabres, M. Ferrando-Bataller, and E. T. Salonen, "Improved planar wideband antenna element and its usage in a mobile MIMO system," *IEEE Antennas Wireless Propag. Lett.*, vol. 11, pp. 826–829, 2012.
- [35] S. Sun, M. Cheng, S. Lu, and J. Lin, "Compact MIMO PIFA for LTE/WWAN operation in the mobile application," in *Proc. 3rd Asia-Pacific Conf. Antennas Propag. (APCAP)*, no. 36, Jul. 2014, pp. 26–28.
- [36] A. Cihangir, F. Ferrero, G. Jacquemod, P. Brachat, and C. Luxey, "Neutralized coupling elements for MIMO operation in 4G mobile terminals," *IEEE Antennas Wireless Propag. Lett.*, vol. 13, pp. 141–144, 2014.
- [37] W.-A. Li, Z.-H. Tu, and Q.-X. Chu, "Design of planar wideband MIMO antenna for mobile phones," in *Proc. IEEE Int. Wireless Symp. (IWS)*, Mar./Apr. 2015, pp. 1–4.
- [38] M. Abdullah, Y.-L. Ban, K. Kang, M.-Y. Li, and M. Amin, "Eight-element antenna array at 3.5 Ghz for MIMO wireless application," *Prog. Electromagn. Res. C*, vol. 78, pp. 209–216, Aug. 2017.
- [39] Y. Wang and Z. Du, "A wideband printed dual-antenna system with a novel neutralization line for mobile terminals," *IEEE Antennas Wireless Propag. Lett.*, vol. 12, pp. 1428–1431, 2013.
- [40] Y. Wang and Z. Du, "A wideband printed dual-antenna with three neutralization lines for mobile terminals," *IEEE Trans. Antennas Propag.*, vol. 62, no. 3, pp. 1495–1500, Mar. 2014.
- [41] A. Akdagli and A. Toktas, "Wideband MIMO antenna with enhanced isolation for LTE, WiMAX and WLAN mobile handsets," *Electron. Lett.*, vol. 50, no. 10, pp. 723–724, May 2014.
- [42] S. S. Alja'afreh, Y. Huang, Q. Xu, L. Xing, and O. A. Saraereh, "MIMO antenna system of a compact 4-element PIFA for 4G handset applications," in *Proc. Loughborough Antennas Propag. Conf. (LAPC)*, Nov. 2016, pp. 1–4.
- [43] H. Huang and J. Wu, "Decoupled dual-antenna with three slots and a connecting line for mobile terminals," *IEEE Antennas Wireless Propag. Lett.*, vol. 14, pp. 1730–1733, 2015.
- [44] Y. Wang and Z. Du, "A printed dual-antenna system operating in the GSM1800/GSM1900/UMTS/LTE2300/LTE2500/ 2.4-GHz WLAN bands for mobile terminals," *IEEE Antennas Wireless Propag. Lett.*, vol. 13, pp. 233–236, 2014.
- [45] Y. Wang and Z. Du, "A wideband printed dual-antenna with a protruded ground for mobile terminals," in *Proc. Antennas Propag. Soc. Int. Symp. (APSURSI)*, Jul. 2014, pp. 1133–1134.
- [46] S. Xu, M. Zhang, H. Wen, and J. Wang, "Deep-subwavelength decoupling for MIMO antennas in mobile handsets with singular medium," *Sci. Rep.*, vol. 7, no. 1, 2017, Art. no. 12162.
- [47] E. Foroozanfard, E. De Carvalho, and G. F. Pedersen, "Design and evaluation of full-duplex terminal antennas in realistic user scenarios," *IEEE Antennas Wireless Propag. Lett.*, vol. 16, pp. 1851–1854, 2017.
- [48] S. Zhang, B. K. Lau, Y. Tan, Z. Ying, and S. He, "Mutual coupling reduction of two PIFAs with a T-shape slot impedance transformer for MIMO mobile terminals," *IEEE Trans. Antennas Propag.*, vol. 60, no. 3, pp. 1521–1531, Mar. 2012.
- [49] J.-N. Lee, K.-C. Lee, N.-H. Park, and J.-K. Park, "Design of dual-band MIMO antenna with high isolation for WLAN mobile terminal," *ETRI J.*, vol. 35, no. 2, pp. 177–187, 2013.
- [50] M. Ikram, R. Hussain, and M. S. Sharawi, "A 4G MIMO antenna system with dual function ground slots," in *5th Asia-Pacific Conf. Antennas Propag. (APCAP)*, vol. 3, 2016, pp. 199–200.
- [51] G. Li, H. Zhai, Z. Ma, C. Liang, R. Yu, and S. Liu, "Isolation-improved dual-band MIMO antenna array for LTE/WiMAX mobile terminals," *IEEE Antennas Wireless Propag. Lett.*, vol. 13, pp. 1128–1131, 2014.
- [52] M. A. Jan, D. N. Aloï, and M. S. Sharawi, "A 2×1 compact dual band MIMO antenna system for wireless handheld terminals," in *Proc. IEEE Radio Wireless Symp. (RWS)*, Jan. 2012, pp. 23–26.
- [53] M. S. Sharawi, A. B. Numan, M. U. Khan, and D. N. Aloï, "A dual-element dual-band MIMO antenna system with enhanced isolation for mobile terminals," *IEEE Antennas Wireless Propag. Lett.*, vol. 11, pp. 1006–1009, 2012.
- [54] K. Wang and T. F. Eibert, "Low profile dual band WLAN antenna array for mobile terminals," in *Proc. IEEE Int. Symp. Antennas Propag. USNC/URSI Nat. Radio Sci. Meeting*, Jul. 2015, pp. 378–379.
- [55] C.-Y. Chiu, S. Shen, and R. D. Murch, "Dual-band antenna pair for MIMO WiFi compact mobile terminals," in *Proc. IEEE Int. Symp. Antennas Propag. (APSURSI)*, Jun./Jul. 2016, pp. 65–66.
- [56] D. Wu, S. W. Cheung, T. I. Yuk, and X. L. Sun, "A MIMO antenna for mobile applications," in *Proc. Int. Workshop Antenna Technol. (iWAT)*, no. 1, Mar. 2013, pp. 87–90.
- [57] W. J. Krzysztolik, "Space diversity parameters of MIMO systems small antenna array for mobile terminal," in *Proc. 10th Eur. Conf. Antennas Propag. (EuCAP)*, Apr. 2016, pp. 1–4.
- [58] S. Shoaib, I. Shoaib, X. Chen, and C. G. Parini, "MIMO antennas for next generation mobile terminals," in *Proc. 10th Eur. Conf. Antennas Propag. (EuCAP)*, Apr. 2016, pp. 1–4.
- [59] X. Zhao and J. Choi, "Multiband MIMO antenna for 4G mobile terminal," in *Proc. Asia-Pacific Microw. Conf. (APMC)*, Nov. 2013, pp. 49–51.
- [60] S. Shoaib, I. Shoaib, N. Shoaib, X. Chen, and C. G. Parini, "Design and performance study of a dual-element multiband printed monopole antenna array for MIMO terminals," *IEEE Antennas Wireless Propag. Lett.*, vol. 13, pp. 329–332, 2014.
- [61] H. Huang and J.-F. Wu, "Decoupled hepta-band antenna array with three slots for WWAN/LTE mobile terminals," in *Proc. Asia-Pacific Microw. Conf. (APMC)*, vol. 7, Dec. 2015, pp. 1–3.
- [62] Q. Sun, B. Sun, L. Sun, W. Huang, and Q. Ren, "Broadband two-element array with hybrid decoupling structures for multimode mobile terminals," *IEEE Antennas Wireless Propag. Lett.*, vol. 14, pp. 1431–1434, 2015.
- [63] X. Chen, S. Zhang, and Q. Li, "A review of mutual coupling in MIMO systems," *IEEE Access*, vol. 6, pp. 24706–24719, 2018.
- [64] Y. L. Ban, Y. F. Qiang, Z. Chen, K. Kang, and J. H. Guo, "A dual-loop antenna design for hepta-band WWAN/LTE metal-rimmed smartphone applications," *IEEE Trans. Antennas Propag.*, vol. 63, no. 1, pp. 48–58, Jan. 2015.
- [65] Y. Yan, Y.-L. Ban, G. Wu, and C.-Y.-D. Sim, "Dual-loop antenna with band-stop matching circuit for WWAN/LTE full metal-rimmed smartphone application," *IET Microw., Antennas Propag.*, vol. 10, no. 15, pp. 1715–1720, 2016.
- [66] L.-W. Zhang, Y.-L. Ban, C.-Y.-D. Sim, J. Guo, and Z.-F. Yu, "Parallel dual-loop antenna for WWAN/LTE metal-rimmed smartphone," *IEEE Trans. Antennas Propag.*, vol. 66, no. 3, pp. 1217–1226, Mar. 2018.
- [67] J.-W. Lian, Y.-L. Ban, Y.-L. Yang, L.-W. Zhang, C.-Y.-D. Sim, and K. Kang, "Hybrid multi-mode narrow-frame antenna for WWAN/LTE metal-rimmed smartphone applications," *IEEE Access*, vol. 4, pp. 3991–3998, 2016.
- [68] Y. Liu, Y.-M. Zhou, G.-F. Liu, and S.-X. Gong, "Heptaband inverted-F antenna for metal-rimmed mobile phone applications," *IEEE Antennas Wireless Propag. Lett.*, vol. 15, pp. 996–999, 2016.
- [69] Y.-L. Ban, Y.-F. Qiang, G. Wu, H. Wang, and K.-L. Wong, "Reconfigurable narrow-frame antenna for LTE/WWAN metal-rimmed smartphone applications," *IET Microw. Antennas Propag.*, vol. 10, no. 10, pp. 1092–1100, Apr. 2016.

- [70] H. Chen and A. Zhao, "LTE antenna design for mobile phone with metal frame," *IEEE Antennas Wireless Propag. Lett.*, vol. 15, pp. 1462–1465, 2016.
- [71] M. Stanley, Y. Huang, H. Wang, H. Zhou, Z. Tian, and Q. Xu, "A novel reconfigurable metal rim integrated open slot antenna for octa-band smartphone applications," *IEEE Trans. Antennas Propag.*, vol. 65, no. 7, pp. 3352–3363, Jul. 2017.
- [72] T. S. Rappaport, J. N. Murdock, and F. Gutierrez, Jr., "State of the art in 60-GHz integrated circuits and systems for wireless communications," *Proc. IEEE*, vol. 99, no. 8, pp. 1390–1436, Aug. 2011.
- [73] T. S. Rappaport et al., "Millimeter wave mobile communications for 5G cellular: It will work!" *IEEE Access*, vol. 1, pp. 335–349, May 2013.
- [74] I. Chih-Lin, C. Rowell, S. Han, Z. Xu, G. Li, and Z. Pan, "Toward green and soft: A 5G perspective," *IEEE Commun. Mag.*, vol. 52, no. 2, pp. 66–73, Feb. 2014.
- [75] H. W. Lai and H. Wong, "Substrate integrated magneto-electric dipole antenna for 5G Wi-Fi," *IEEE Trans. Antennas Propag.*, vol. 63, no. 2, pp. 870–874, Feb. 2014.
- [76] M. A. U. Haq, M. A. Khan, and M. R. Islam, "MIMO antenna design for future 5G wireless communication systems," in *Software Engineering, Artificial Intelligence, Networking and Parallel/Distributed Computing*. Cham, Switzerland: Springer, 2016, pp. 175–183.
- [77] K. M. Mak, H. W. Lai, K. M. Luk, and C. H. Chan, "Circularly polarized patch antenna for future 5G mobile phones," *IEEE Access*, vol. 2, pp. 1521–1529, 2014.
- [78] M.-Y. Li et al., "Eight-port orthogonally dual-polarized antenna array for 5G smartphone applications," *IEEE Trans. Antennas Propag.*, vol. 64, no. 9, pp. 3820–3830, Sep. 2016.
- [79] M.-Y. Li, Z.-Q. Xu, Y.-L. Ban, C.-Y.-D. Sim, and Z.-F. Yu, "Eight-port orthogonally dual-polarized MIMO antennas using loop structures for 5G smartphone," *IET Microw., Antennas Propag.*, vol. 11, no. 12, pp. 1810–1816, Sep. 2017.
- [80] Z. Qin, W. Geyi, M. Zhang, and J. Wang, "Printed eight-element MIMO system for compact and thin 5G mobile handset," *Electron. Lett.*, vol. 52, no. 6, pp. 416–418, Mar. 2016.
- [81] Y.-L. Ban, C. Li, C.-Y.-D. Sim, G. Wu, and K.-L. Wong, "4G/5G multiple antennas for future multi-mode smartphone applications," *IEEE Access*, vol. 4, pp. 2981–2988, 2016.
- [82] M. Abdullah, Y.-L. Ban, K. Kang, O. K. K. F. Sarkodie, and M.-Y. Li, "Compact 4-port MIMO antenna system for 5G mobile terminal," in *Proc. Int. Appl. Comput. Electromagn. Soc. Symp. (ACES)*, Florence, Italy, vol. 1, Mar. 2017, pp. 1–2.
- [83] M.-Y. Li, Y.-L. Ban, Z.-Q. Xu, J. Guo, and Z.-F. Yu, "Tri-polarized 12-antenna MIMO array for future 5G smartphone applications," *IEEE Access*, vol. 6, pp. 6160–6170, 2017.
- [84] Y. Qi et al., "5G over-the-air measurement challenges: Overview," *IEEE Trans. Electromagn. Compat.*, vol. 59, no. 6, pp. 1661–1670, Dec. 2017.
- [85] P.-D. V. Domingo and L.-P. Ridel, "Design of a dual-band PIFA for handset devices and its SAR evaluation," *Ingeniería, Investigación y Tecnología*, vol. 17, no. 2, pp. 169–178, Apr./Jun. 2016.
- [86] R. Khan, A. A. Al-Hadi, and P. J. Soh, "Recent advancements in user effect mitigation for mobile terminal antennas: A review," *IEEE Trans. Electromagn. Compat.*, vol. 61, no. 1, pp. 279–287, Feb. 2019.
- [87] Y. Li, C.-Y.-D. Sim, Y. Luo, and G. Yang, "12-port 5G massive MIMO antenna array in sub-6GHz mobile handset for LTE bands 42/43/46 applications," *IEEE Access*, vol. 6, pp. 344–354, 2017.
- [88] H. S. Singh and M. K. Meshram, "Effect of user proximity on internal quad band mobile phone MIMO/diversity antenna performances," *Wireless Pers. Commun.*, vol. 95, no. 2, pp. 1417–1431, 2017.
- [89] C. M. N. C. Isa, A. A. Al-Hadi, S. N. Azemi, A. M. Ezanuddin, H. Lago, and M. F. Jamlos, "Effects of hand on the performance of 5 GHz two-port terminal antennas," in *Proc. IEEE Asia-Pacific Conf. Appl. Electromagn. (APACE)*, Dec. 2016, pp. 207–210.
- [90] I. Syrytsin, S. Zhang, and G. F. Pedersen, "Performance investigation of a mobile terminal phased array with user effects at 3.5 GHz for LTE advanced," *IEEE Antennas Wireless Propag. Lett.*, vol. 16, pp. 1847–1850, 2016.
- [91] C. Di Paola, I. Syrytsin, S. Zhang, and G. F. Pedersen, "Investigation of user effects on mobile phased antenna array from 5 to 6 GHz," in *Proc. 12th Eur. Conf. Antenna Propag. (EuCAP)*, Apr. 2018, pp. 1–5.
- [92] R. Tian, B. K. Lau, and Z. Ying, "Multiplexing efficiency of MIMO antennas with user effects," in *Proc. Int. Symp. Antennas Propag. Soc.*, Jul. 2012, pp. 1–2.



**RIZWAN KHAN** (S'15) was born in Abbottabad, Pakistan, in 1990. He received the M.S. degree in electrical engineering from the COMSATS Institute of Information Technology, Abbottabad, in 2015, and the Ph.D. degree in communication engineering from Universiti Malaysia Perlis (UniMAP), Malaysia, in 2018. From 2015 to 2016, he was served on COMSATS as a Research Associate with the Department of Electrical Engineering. He is currently a Researcher at the Advanced Communication Engineering Center, UniMAP. He has published several impact factor journals, and national and international conference papers. His research interests include mobile terminal antennas and their user interactions, MIMO antennas, dielectric resonator antennas, metamaterial, electrically small antenna, and reconfigurable antennas.



**AZREMI ABDULLAH AL-HADI** (S'13–M'13–SM'14) was born in Michigan, USA. He received the M.Sc. degree in communication engineering from Birmingham University, U.K., in 2004, and the Doctor of Science in Technology degree from Aalto University, Finland, in 2013. His current research interests include the design and performance evaluation of multi-element antennas, mobile terminal antennas and their user interactions, and wireless propagation.

He is currently an Associate Professor and the Dean of the School of Computer and Communication Engineering, Universiti Malaysia Perlis (UniMAP), where he has been with the school since 2002. He is active in volunteer work with the IEEE Malaysia Section, acting as the Vice Chair of the IEEE Antenna Propagation/Microwave Theory Techniques/Electromagnetic Compatibility Malaysia Chapter and a Counselor for the IEEE UniMAP Student Branch. He is the Chartered Engineer of the Institution of Engineering and Technology, U.K., the member of the Board of Engineers Malaysia, and a Malaysia and Graduate Technologist of the Malaysia Board of Technologist, Malaysia. Dr. Al-Hadi was a recipient of the Best Student Paper Award presented at the 5th Loughborough Antennas and Propagation Conference in 2009 and the CST University Publication Award in 2011.



**PING JACK SOH** (S'10–M'14–SM'15) was born in Kota Kinabalu, Sabah, Malaysia. He received the B.Eng. and M.Eng. degrees in electrical engineering (telecommunication) from Universiti Teknologi Malaysia in 2002 and 2006, respectively, and the Ph.D. degree in electrical engineering from KU Leuven, Belgium, in 2013.

He is currently an Associate Professor at the School of Computer and Communication Engineering (SCCE), Universiti Malaysia Perlis (UniMAP), and also a Research Affiliate at KU Leuven. From 2002 to 2004, he was a Test Engineer at Venture Corporation Ltd. In 2005, he joined Motorola Solutions Malaysia as an R&D Engineer, where he was worked on the characterization and testing of new two-way radios' antennas and RF front-ends. In 2006, he joined SCCE-UniMAP as a Lecturer, and also served as the Deputy Director of the Centre for Industrial Collaboration from 2007 to 2009. He went on leave from UniMAP in 2009 to pursue his Ph.D. degree and research attachment in KU Leuven. First, he was a Research Assistant (2009–2013), then a Post-Doctoral Research Fellow (2013–2014), and is currently a Research Affiliate with the ESAT-TELEMIC Research Division. His involvement in several industrial research projects such as with AGFA Healthcare Belgium resulted in a granted patent and five other filed patents. Upon his return to UniMAP, he resumed his role as a Senior Lecturer and, concurrently, served as the Deputy Dean of the University's Research Management and Innovation Center from 2014 to 2017. He researches actively in his areas of interest: wearable antennas, arrays, metasurfaces; on-body communication; electromagnetic safety and absorption; and wireless and radar techniques for healthcare applications. To date, he has lead/is leading six internationally and nationally funded projects, besides being involved collaboratively in other projects.

Dr. Soh is a Chartered Engineer registered with the U.K. Engineering Council, a Professional Technologist registered with the Malaysia Board of Technologist, and a member of IET, ACES, and URSI. He was a recipient of the IEEE Antennas and Propagation Society (AP-S) Doctoral Research Award in 2012, the IEEE Microwave Theory and Techniques Society (MTT-S) Graduate Fellowship for Medical Applications in 2013, and the International Union of Radio Science (URSI) Young Scientist Award in 2015. He was also the Second Place Winner of the IEEE Presidents' Change the World Competition and the IEEE MTT-S Video Competition in 2013. Two of his co-authored journals were also awarded the CST University Publication Award in 2011 and 2012. As a Project Advisor, his supervised students have also received prizes, such as the First Place in the IEEE Malaysia Section Final Year Project Competition (Telecommunication Track) in 2015, the First Place in the Innovate Malaysia Design Competition (Motorola Track) in 2016, and the IEEE MTT-S Undergraduate Scholarship in 2016. He also serves in the IEEE MTT-S Education Committee and the IEEE MTT-S Meetings and Symposia Committee.



**MUHAMMAD RAMLEE KAMARUDIN** (M'08–SM'13) received the degree (Hons.) in electrical and telecommunication engineering from the Universiti Teknologi Malaysia, Johor Bahru, Malaysia, in 2003, and the M.Sc. degree in communication engineering and the Ph.D. degree in electrical engineering from the University of Birmingham, Birmingham, U.K., in 2004 and 2007, respectively, under the supervision of Emeritus Prof. P. Hall. He has been a Senior Lecturer with

the Centre for Electronic Warfare, Information and Cyber, Cranfield Defence and Security, Cranfield University, U.K., since 2017. He was an Associate Professor with the Wireless Communication Centre, Universiti Teknologi Malaysia. He holds an H-index of 21 (SCOPUS) and over 1750 citations (SCOPUS). He has authored a book chapter of a book *Antennas and Propagation for Body-Centric Wireless Communications* and has published over 220 technical papers in journals and proceedings, including the IEEE TRANSACTION ON ANTENNAS AND PROPAGATION, the IEEE ANTENNAS AND WIRELESS PROPAGATION LETTER, the *IEEE Antenna Magazine*, the IEEE ACCESS, the *International Journal of Antennas and Propagation*, *Progress in Electromagnetic Research, Microwave and Optical Technology Letters*, and *Electronics Letters*. His research interests include antenna design for 5G, MIMO antennas, array antenna for beam-forming and beam steering, wireless on-body communications, in-body communications (implantable antenna), RF and microwave communication systems, and antenna diversity. He is a member of IET, an Executive Member of Antenna and Propagation, Malaysia Chapter, and a member of the IEEE Antennas and Propagation Society, the IEEE Communication Society, the IEEE Microwave Theory and Techniques Society, the IEEE Electromagnetic Compatibility Society, an Associate Editor of *Electronics Letters* and *IET Microwaves, Antennas and Propagation*, and an Academic Editor of the *International Journal of Antennas and Propagation*.



**MOHD TARMIZI ALI** (M'06–SM'17) received the B.Eng. degree in electrical engineering from Universiti Teknologi Mara (UiTM), Shah Alam, Malaysia, in 1996, the M.Sc. degree in electrical engineering from the University of Leeds, Leeds, U.K., in 2002, and the Ph.D. degree in electrical engineering from the Universiti Teknologi Malaysia, Johor, Malaysia, in 2010. Since 2018, he has been a Professor with the Faculty of Electrical Engineering (FKE), UiTM, where he has also been the Group Leader of the Antenna Research Group since 2011. He has authored over 100 journal papers and conferences proceedings on various topics related to antennas, microwaves, and electromagnetic radiation analysis. He has also filed five patent applications on communication antennas. To date, his publications have been cited 237 times with the H-index of 8 (Source: Google Scholar). He is a member of the Antenna Propagation/Microwave Theory and Technology/Electromagnetic Compatibility Joint Chapter. He was the Chair and a Technical Program Chair of the IEEE Symposium on Wireless Technology and Applications, from 2011 to 2012.



**OWAIS** received the B.E. and master's degrees from the University of Engineering and Technology, Peshawar, Pakistan, in 1996 and 2000, respectively, and the Ph.D. degree in communication electronics from the Department of Science and Technology, Linköping University, Sweden. He has authored 40 international journal articles and awarded a U.S. patent 201110074638 A1 on the design of an Ultra-Wide Band Secondary Antennas and Wireless Devices Using the Same.

He is currently serving as an Associate Professor with the COMSATS University Islamabad, Abbotabad Campus, Pakistan. His main research interests include the design of microstrip patch and dielectric resonator antennas, MIMO and reconfigurable DRAs, electromagnetic band gap, and double negative metamaterials; moreover, sixport front-end circuits for direct conversion transceiver design and high-speed data transmissions are also his area of interest.

• • •